Quartz crystal microbalance and its applications in low temperature physics

Master's thesis
University of Turku
Department of Physics and Astronomy
Physics
2012
B.Sc Ville Virtanen
Tarkastajat:
Doc. Sergey Vasiliev
Prof. Kurt Gloos

TURUN YLIOPISTO
Fysiikan ja tähtieteen laitos

VIRTANEN, VILLE Quartz crystal microbalance and its applications in low temperature physics

Pro Gradu, 69s., 5 liites.
Fysiikka
Toukokuu 2012

Tutkielmassa perehdytään pietsosähköisiin kvartsiresonaattoreihin ja niiden käyttöön mikrovaakana matalissa lämpötiloissa. Aluksi tutustutaan kvartsiresonaattoreiden teoriaan ja sovelluksiin. Seuraavaksi tarkastallaan resonaattoreiden ominaisuuksia kokeellisesti huoneenlämpötilassa ja matalissa lämpötiloissa. Kokeellisen osion alussa on johdanto koelaitteistoon huoneenlämpötilassa ja matalissa lämpötiloissa. Työn päätavoiteena on ollut uuden koelaitteiston rakentaminen atomisen vedyn (H) tutkimiseen kiinteän molekylaarisen vedyn (H_2) sisällä. Koelaitteisto mahdollistaa suprajuoksevan (suprakiinteän) käytöksen etsimisen matalissa lämpötiloissa. Suprajuoksevuus voidaan todeta resonanssitaajuuden kasvusta. Aineen kondensoiminen kvartsin pinnalle aiheuttaa resonanssitaajuuden siirtymisen päinvastaiseen suuntaan.

Kvartsiresonaattorien käyttö mikrovaakoina sai alkunsa vuonna 1959 kun resonanssitaajuuden siirtymä massan funktiona pystyttiin määrittämään tarkasti. Sitä ennen kvartsiresonaattorit toimivat radiotekniikassa taajuuslähteinä ja suodattimina. Vielä nykyäänkin kvartsiresonaattoreita käytetään radiotekniikassa niiden suuren stabiilisuuden vuoksi. Ensimmäinen havainto suprajuoksevuudesta ohuissa helium-kalvoissa tehtiin kvartsiresonaattoreiden avulla 1970-luvulla. Nykyään kvartsiresonaattoreita käytetään monipuolisesti myös muun muassa lääketieteessä ja ohutkalvojen valmistuksessa.

Tutkielmassa rakennetulla koelaitteistolla saavutettiin 0.3 Hz (RMS) stabiilisuus kvartsin resonanssitaajuudessa pitkällä aikavälillä 100 mK lämpötilassa. Vastavasti lyhyellä aikavälillä saavutettiin 0.1 Hz (RMS) stabiilisuus. Tällä tarkkuudella kvartsiresonaattorilla on mahdollista havaita suprakiinteä aineen olomuoto 0.55 μm paksuisessa kiinteässä molekulaarisessa vetykalvossa, mikäli 0.03 % vedystä muuttuu suprajuoksevaksi. Ilmiö voi esiintyä myös atomisessa vedyssä loukkuuntuneena kiinteään molekulaariseen vetymatriisiin. Aikaisemmissa kokeissa atomisen vedyn konsentraatio molekulaarisessa vedyssä on ollut luokkaa 0.1 %, jolloin 0.55 μm paksuisessa molekulaarisessa vetykalvossa on mahdollista havaita suprakiinteäkäytös, mikäli 6 % atomisestä vedystä muuttuu suprajuoksevaksi.

Tutkielman kokeellisessa osiossa kvartsin pinnalle kondensoitiin molekulaarista vetyä, mikä aiheutti 1100 Hz siirtymän resonanssitaajuudessa. Tämä vastaa 0.55 μm paksuista kerrosta molekulaarista vetyä.

Asiasanat: Pietsosähköinen ilmiö, kvartsiresonaattori, mikrovaaka, molekulaarinen vety, suprakiinteä olomuoto

Contents

Acknowledgements

This work has been carried out in the Wihuri Physical Laboratory at the Physics Department of the University of Turku. I want to express my sincere gratitude to my supervisor Doc. Sergey Vasiliev for his quidance and vital discussion. I am also grateful for him for giving me the opportunity to work in the reseach group. My special gratitude goes to Dr. Janne Ahokas for his constant support and for teaching me most I know of low temperature physics. I would also thank my present collegue M.Sc. Sergey Shelydyakov for his contribution and for the pleasant working environment.

A would also wish to thank the technical staff of the University, especially Mr. T.Haili for preparing the components needed in our new experiment setup and Mr. Esa Lilja in providing helium.

Turku, May 2012

Ville Virtanen

Introduction

Many physical and chemical processes and phenomena such as thin film growth, adsorption, desorption and oxidation can be followed by simply observing the associated mass changes. However, the accuracy of the mass measurement with conventional devices such as spring balances is poor for small masses. A completely new method for mass measurements was introduced by Sauerbrey [1] in 1959. Instead of measuring the displacement of the spring balance, Sauerbrey used the change of the resonance frequency of the quartz resonator to measure the mass of a film deposited on the surface of the quartz resonator.

The use of quartz crystal microbalances (QCM) as a mass sensor is based on the piezoelectric effect. The application of a mechanical strain results in an electrical potential across the material. In the opposite case, the application of a potential across the material introduces mechanical strain. An alternating potential causes the quartz to oscillate at certain frequency. When the applied voltage is close to one of the mechanical resonances of the quartz the amplitude of the mechanical vibrations reaches a maximum. This frequency is known as the resonance frequency, which depends on the material properties such as thickness of the quartz plate. Adding mass to the surface of the QCM causes a decrease of the resonance frequency due to the increased amount of mass that vibrates. By detecting the change of the resonance frequency the mass deposited on the surface of the QCM can be determined with an accuracy of less than one atomic layer. The accuracy of the mass measurement originates from the accuracy of the smallest change in the frequency which can be detected. Frequency is a quantity which can be determined in the most accurate way. High Q values of QCMs allow to measure the resonance frequency with high accuracy. For this reason QCMs are powerfull tools for detecting even masses of 1 pg/cm^2.

Since its early days quartz resonators have been widely used in high accuracy

timing devices and in electrical circuits to generate or filter radio frequency signals. Due to their small price, high quality factor (small intrinsic damping) and great stability quartz resonators have been found almost irreplaceable. Nowadays quartz microbalances are used in large variety of applications such as in gas phase detection, immunosensors, DNA biosensors, space system contamination studies and aerosol mass measurement [2]. QCM has also proved its power in the research of quantum fluids such as liquid helium. The first study of the onset of superfluidity in thin helium films using QCM was performed in 1972 [3]. The onset of superfluidity can be observed as the resonance frequency increase, because only the normal component remains coupled to the quartz motion.

The chief interest in this thesis is to study the properties of quartz microbalances and their applications in low temperature physics. In particular there is an idea of studying possible superfluid behavior of films of solid molecular hydrogen with embedded H atoms [4]. The superfluid transition may be detected by QCM. We need to evaluate requirements and its ability to detect this phenomenon.

The thesis is organized as follows. The first chapter includes basic information on quartz crystal resonators and their applications for mass measurement. The second chapter describes experiments on quartz crystals at room temperature. In addition it contains detailed information on the electrode manufacturing for bare crystals. The goal of the second chapter is to test crystals from three different manufacturers with different kind of electrode configurations and to choose the best crystal for experiments with atomic hydrogen in solid H_2 matrices. The third chapter includes a description of the structure of the SC and experiments on the performance of the QCM at cryogenic temperatures.

Cryogenic tests of the QCM performance were done in real sample cell mounted inside the dilution refrigerator. We reached 0.3 Hz (RMS) long term and 0.1 Hz (RMS) short term stability of the QCM frequency measured with the excitation

power of -40 dBm. With this stability we will be able to detect superfluid fraction of 2.20×10^{-7} in 250 μm thick H_2 film.

1 Quartz crystal microbalance

1.1 Piezoelectricity

Piezoelectricity is a phenomenon where the charge accumulates in a solid material in response to applied mechanical stress. A crude model of unit cell can be described as an arrangement of positive and negative ions arranged in the plane so that the net charge is zero. During the deformation of the crystal caused by the application of external stresses, the mutual forces acting between the ions in the cell are such as to maintain both the distance apart of opposite pairs of ions. Then the deformation of the unit cell can be described in terms of the rotations of the plane normal lines causing the change of the position of the positive and negative ions so that they produce a non zero change.

The use of quartz crystals as microbalances is based on the piezoelectric property of the quartz. Application of a mechanical strain σ results in the generation of an electrical potential across the crystal, according to the equation (1).

$$D = d\sigma, \tag{1}$$

where D is electrical charge density displacement and d is piezoelectric tensor. This is known as direct piezoelectric effect. Induced electric charge reverses its sign if the stress to the crystal is changed from tensile to compressive. On the contrary the converse piezoelectric effect appears when introducing the application of electrical potential E to the crystal. This induces mechanical strain S, a deformation according to equation (2).

$$S = dE \tag{2}$$

A shear piezoelectric effect is also possible, as it linearly couples shear mechanical stress or strain with the electric charge [5]. Figure 1 illustrates direct, converse and shear piezoelectric effects in longitudinal direction.

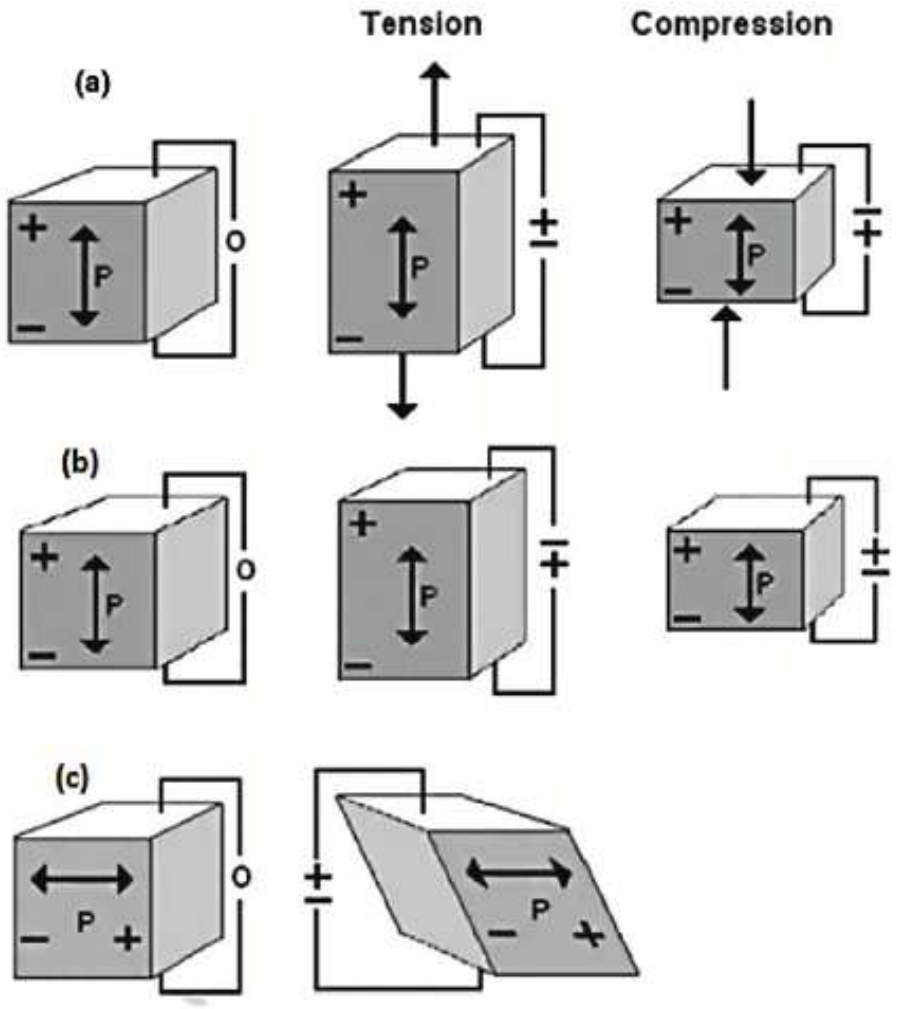

Figure 1. A schematic view of direct (a), converse (b) and shear (c) piezoelectric effects in longnitudal direction [5].

Crystallographic symmetry of materials plays an important role in the piezoelectric phenomenon. Piezoelectricity appears only in insulating crystals which do not possess a center of symmetry [6]. A crystal which has a center of symmetry cannot be piezoelectric, because all components of the piezoelectric tensor vanish [5]. Depending on the symmetry three-dimensional crystals can be divided into 32 different point groups. 20 of these classes own the property of piezoelectricity. Still all of these 20 classes do not necessarily show any sizable piezoelectric effect [7].

1.2 Physical Properties of Quartz

Crystalline quartz is composed of two elements: silicon and oxygen. Its chemical formula is called silicon dioxide (SiO_2). Quartz as a material is hard, fragile and transparent [8]. After H_2O it is found to be the second most abundant molecule on earth. In nature quartz can be found mainly in two different forms known as α-quartz and β-quartz [9]. Sometimes α-quartz is called as low-quartz and β-quartz is called as high-quartz [8]. For resonator applications α-quartz is of interest due to its thermodynamic stability at room temperature [10]. Under atmospheric pressure at 573°C α-quartz changes its crystalline form into β-quartz. If stress is applied the transform temperature can be even lower [6]. In addition to these two phases there exist also polymorphs of SiO_2, which are stable only at very high temperatures [10]. Quartz is insoluble in ordinary acids, however it is soluble in hydrofluoric acid and in alkaline solutions [8].

Unlike in noncrystalline materials the physical properties of crystalline materials are dependent upon the orientation of crystalline axes. The crystals where the physical properties depend on the direction are known as anisotropic crystals. Quartz is anisotropic and one of the fundamental examples of anisotropy is its electrical conductivity, which is 1000 times larger in one direction than in an other. Other anisotropic properties of quartz are for example hardness, thermal conductivity and

dielectric and piezoelectric constants [11].

In crystallography quartz is described as trigonal trapezohedral [6]. α-quartz belongs to the crystallographic class 32. It has a single axis of threefold symmetry known as trigonal axis and perpendicular to this axis there are three axis of twofold symmetry (digonal axes). The digonal axes are called as polar axes and are spaced 120° apart. The presence of polar axes is required for the existence of the piezoelectric effect since they present the lack of a centre of symmetry [8]. The bonding of Si-O is 60 % covalent and 40 % ionic. The average bonding energy is about 4.85 eV. Unit cell lattice constants of α-quartz are a = 0.4913 nm, b = 0.4913 nm and c = 0.5404 nm at room temperature [9]. The melting point of quartz is 1750°C , the density 2.65 g/cm^3 and the hardness 7 on the Mohs's scale. α-quartz is an optically active material, it exist in two optical forms right-hand and left-hand. The difference between right-hand and left-hand is how the crystal will rotate the plane of polarization of polarized light passing along the z-direction [6]. In right-hand quartz the plane of polarization rotates clockwise when one looks towards the light source. On the contrary in left-hand quartz it rotates anti-clockwise [8]. Quartz used in microbalance application is a cut slab from natural or synthetic single crystal quartz. In figure 2 a right-hand quartz and its symmetry axes with its natural facets is shown.

1.2.1 Quartz manufacturing

Most of the quartz for microbalance application is produced synthetically. This is because the quality factor Q, which presents the intrinsic acoustic losses of the crystal, is too low due to impurities in natural quartz. The smaller are the acoustic losses of the crystal, - the higher is the quality factor [10]. Another reason to use synthetically produced quartz is the limited supply and the high cost of natural quartz [11].

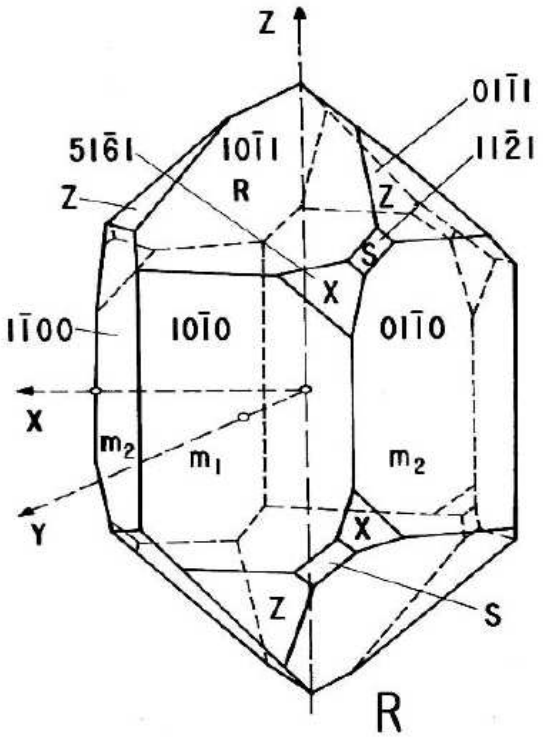

Figure 2. Right-hand quartz and its symmetry axes with its natural facets [7].

The growing method of quartz crystal is called hydrothermal qrowth process. The growing process is placed in steel pressure vessel called autoclave, where synthetic quartz is grown by dissolving SiO_2 in alkaline solution at high temperatures. Typical solutions are NaOH and Na_2CO_3 [10]. The quality of the quartz depends upon the conditions of growth. The slower the growth, the higher the quality [11].

1.2.2 Defects in quartz

Even the finest sythetical crystals include defects and impurities, which limit the quality factor of quartz. Defects can be dislocations, grain boundaries and gross defects like twins. Twins can be created and moved by mechanical and thermal stresses. In addition to lower Q factor the crystals with high defect density can also be more fragile. The most common impurities in synthetically grown and in natural quartz are hydrogen atoms, which are usually present as OH at O sites. Other impurities can be, for example, lithium, aluminium, copper and sodium. These impurities can appear either in substitutional or interstitial sites. The position of the impurities influences electrical and mechanical losses at high frequency [10]. It is shown in ref.[10] that the quality factor is reduced by a factor of two when hydrogen concentration is doubled. Instead of the normal quality factor, quartz can be characterized in terms of the infrared quality factor (Q_{inf}) which is inversely proportional to the hydrogen content [10].

Information on impurities in quartz can be obtained from infrared absorption spectroscopy. Certain impurities can be identified by peaks at the wavelength characteristic to these impurities. Also electron spin resonance (ESR) is used to study impurity atoms like hydrogen and copper [12].

Quartz can be purified by the application of a strong electric field (1kV/cm) at high temperature (500°C). In the strong electric field charged ions such as Li^+ and Na^+ can be removed. This can be made in air or in H_2. In H_2 ions are replaced by

hydrogen atoms [12].

1.3 Quartz crystal resonator

Compared to other resonators such as LC circuits or mechanical resonators the quartz resonator has superior advantages. The material properties are extremely stable and the acoustic loss or internal friction is remarkably small, which leads to extremely high quality factor usually from several thousand to few hundred thousands at room temperatures allowing to measure the frequency of the quartz resonator in a very accurate way [8].

Quartz crystal resonators were used first in radio-communication equiments. It was known that a material deposit on the surface of the quartz crystal changes the resonance frequency [13]. Until 1959 the relation between resonance frequency and deposited mass was not perfectly know. Then Sauerbrey introduced a quantitative relationship (3).

$$\Delta f = -\frac{2f_q^2}{\rho_q v_q} m_f, \tag{3}$$

where Δf is the frequency change, f_q is the resonance frequency of the quartz resonator, ρ_q the density of the quartz, v_q the transversal (shear) wave velocity and m_f is areal density of deposited material [1]. The factor of two in equation (3) accounts for deposition of material on both of the two faces of quartz [3].

After this a microbalance became one of the fundamental application of quartz crystals. A piezoelectric quartz crystal resonator used in microbalances is a thin quartz disk with electrodes fixed on its surfaces [2]. Circular plates have several advantages over rectangular plates including ease of production and are preferred for most applications [11]. When the electrodes are connected to a periodic voltage source the QCM vibrates at the frequency of the excitation voltage. The amplitude of the mechanical vibration reaches a maximum when the frequency of the driving voltage is close to one of the mechanical resonances of the quartz crystal. This is

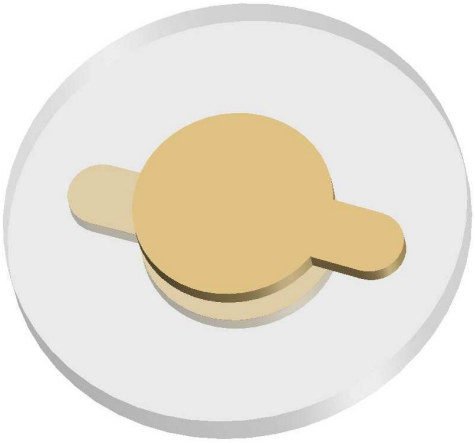

Figure 3. Schematic of a Typical QCM.

known as resonance frequency of the QCM [7]. Figure 3 presents a schematic picture of a typical QCM with key-shaped electrodes. Resonance frequency depends on the physical properties of quartz like chemical structure, disk shape and the total mass of the vibrating body, but one of the most important factors determining the resonance frequency is the thickness of the quartz disk. The thickness also determines the mass sensitivity. The thinner the plate is, the higher is QCM's sensitivity and resonance frequency, but consequently quartz becomes more fragile [2]. A rule of thumb in determining QCM frequency is that when the thickness of the quartz disk is halved the resonance frequency is doubled [7].

1.4 Vibration modes

In an infinite solid three types of waves can be exited. One longitudinal and two transversal modes [10]. The QCM mode of vibration which is most sensitive to the addition or removal of mass is the high frequency thickness-shear mode, where the two main surfaces of the QCM move in the opposite direction with respect to each

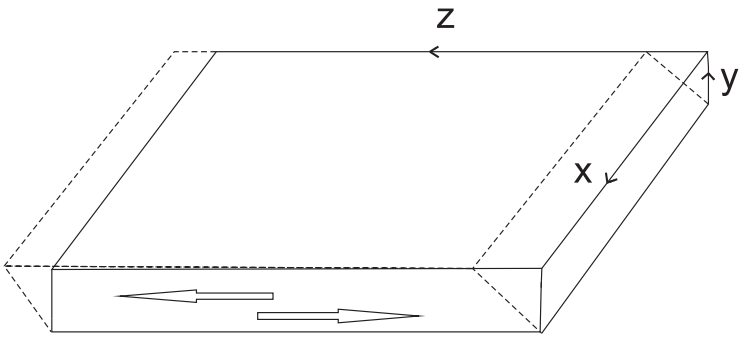

Figure 4. Thickness-shear mode vibration.

other [7]. The thickness-shear mode vibration is illustated in figure 4. In addition to the fundamental modes the system can also vibrate at the overtones of each fundamental mode. Modes can also couple to each other, and in that way they can form very complicated resonances [7].

Mathematically the thickness-shear modes can be approximated by a single displacement u. In cartesian coordinate system with y-axis normal to the plate of the resonator, the x-axis parallel to the plate, the displacement can be written as

$$u = A(x, z)sin(ky)sin(\omega t), \tag{4}$$

where A is the amplitude of the shear wave, k is the wavenumber and ω is the angular frequency. ω is related to k via the dispersion law ($\omega = v_q k$). When A is a constant, equation (4) describes a standing shear wave reflecting from the surfaces of an infinite flat crystal. In this situation the wavenumber k takes values $n\pi/b$ where n is the number of harmonic overtone (n = 1,3,5,...) and b is the thickness of the crystal. However for a finite-size crystal A is not a constant. The various A possible for each value of n defines the harmonic overtone modes, each of which is characterized by a resonance frequency [14].

The resonance frequency of the quartz plate can be written as

$$f_n = n\frac{v_q}{2d_q}, \tag{5}$$

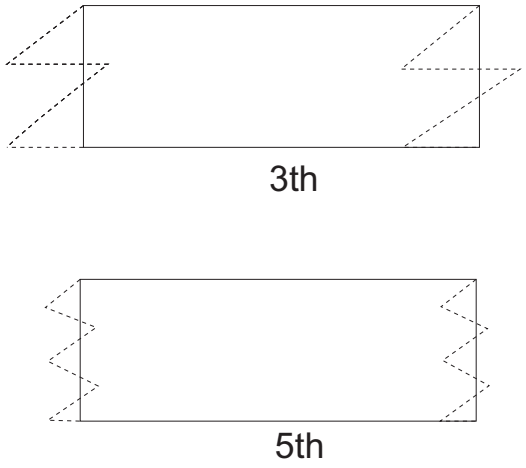

Figure 5. 3rd and 5th overtone modes.

where v is the velocity of sound and d_q is the plate thickness. The harmonic number n can get only odd values, because even harmonics cannot be excited under symmetric load conditions. The next harmonic after fundamental is when $n = 3$ and this mode is named as the third harmonic, next is the fifth harmonic ($n = 5$) and so on [15]. Actually the frequencies of the harmonics are not related as precisely integers due to differences between the vibrating areas and the plated areas in different modes [11]. Typical resonance frequency in fundamental mode is in the range 1 - 30 MHz, for third harmonic 30 - 90 MHz and for fifth harmonic 60-150 MHz [16]. Figure 5 represents 3rd and 5th overtones in thickness-shear mode.

1.5 Quartz plate cuts

A cut with respect to a certain crystallographic axis will strongly affect the resonance properties of QCM. To make QCM oscillate in the thickness-shear mode and to suppress all unwanted modes, the plate must be cut to a specific orientation with respect to the crystal axes [7]. First quartz resonators were cut in such a way that the normal to the plate is parallel to crystal's X-axis. Nowadays Y-cut crystals have replaced X-cut crystals because they have fewer unwanted modes of vibration and they are less affected by air damping [11].

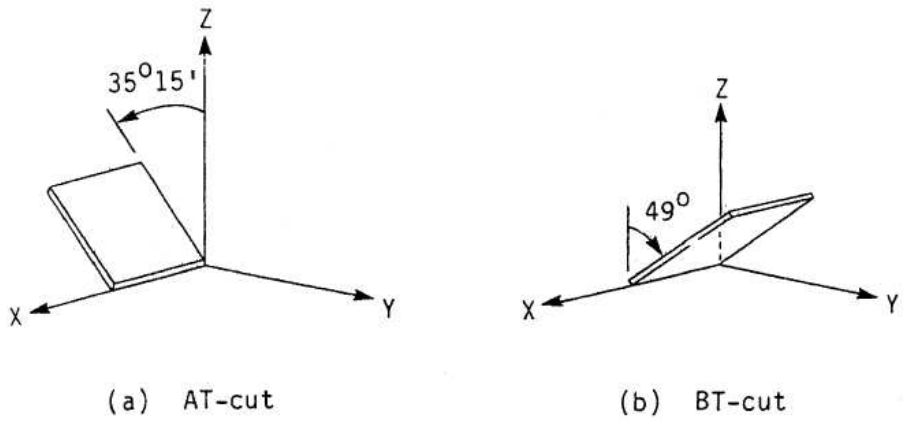

Figure 6. AT- and BT-cut crystals [2].

In standard notation the orientation of Y-cut crystal is described by (yxl)Φ, where the first and second letters describe the directions of the two important dimensions of the plate with references to the capital axes. The first one describes the thickness, the second is for the length and the third is for the width. The angle Φ is determined between Z-axis and the crystal plane and it is positive for counterclockwise rotation. The most widely used Y-cut crystal is known as AT-cut which has Φ = 35°15' [7]. Another widely used cut is called BT-cut, which has Φ = 49°. There exist also other plate cuts like DT-, FC and RT-cuts, but mainly AT-cut crystals are used as microbalances, because of their temperature insensitivity at room temperature [15]. Recently, interest towards the resonator of doubly rotated Y-cut has increased due to its smaller sensitivity to thermal shock and mechanical stress. This type of cut is called as SC-cut [7]. Figure 6 presents AT- and BT-cut quartz crystal plates.

1.5.1 Frequency-Temperature characteristics

Equation (5) may also be written in different form if we know that the velocity of propagation of a shear wave is

$$v = \sqrt{\frac{c_{ij}}{\rho}}, \tag{6}$$

where c_{ij} is the elastic constant equal to the ration of the stress to the strain associated with the elastic wave which propagates in the quartz and ρ is the density of quartz. Now the resonance frequency can be written as

$$f_n = \frac{n}{2d}\sqrt{\frac{c_{ij}}{\rho}} \tag{7}$$

The resonance frequency of the QCM depends on the thickness, density and the elastic constant of the quartz and each of these will change with the temperature. Then the resonance frequency is also temperature dependent [11].

The frequency-temperature characteristics for AT- and BT-cut crystals can be described by a power series of the temperature known as Bechmann's expression

$$(f - f_0)/f_0 = a(T - T_0) + b(T - T_0)^2 + c(T - T_0)^3, \tag{8}$$

where f is the frequency at a temperature T and f_0 is the frequency at the reference temperature T_0. The coefficients a, b and c can be expressed as linear functions of the angle increase

$$a = a_0 + a_1\Delta\theta$$

For AT- and BT-cut crystals the magnitude of the terms in equation (8) is found to be different. For AT-cut the cubic term dominates and gives S shaped frequency-temperature characteristics. On the other hand for BT-cut crystals the quadratic term dominates, which gives a parabolic frequency temperature characteristics [8]. Figures 7 and 8 represent frequency-temperature characteristics for AT- and BT-cut crystals. For standard AT-cut crystal the resonance frequency is insensitive to the temperature change at room temperature. This is one reason why AT-cut crystals are well-trodden in many applications. It has also been found that Y-cut crystal with

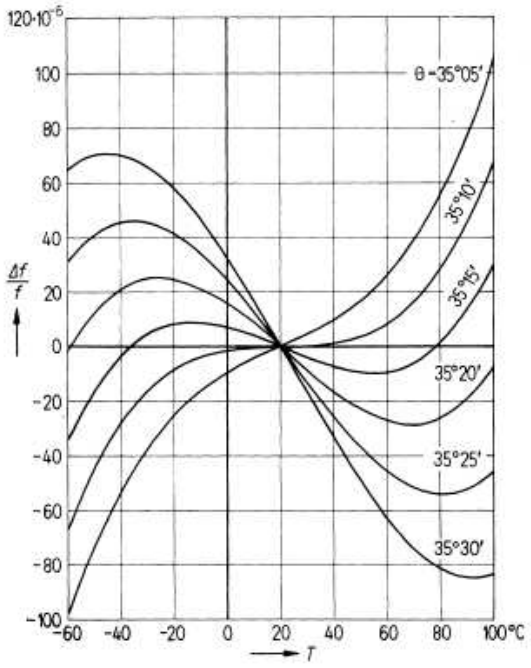

Figure 7. Frequency-temperature characteristics of AT-cut crystal [17].

$\Phi = 41°10'$ has minimized temperature dependence at liquid helium temperatures [7].

1.6 Equivalent electrical circuits

Equivalent circuits refers to a theoretical circuits that retain all of the electrical properties of material. Usually equivalent circuits are simplifications so they describe the properties of the material only in ideal situations. If all unwanted modes of vibration near the resonance can be suppressed then the resonance of QCM can be represented by the simple equivalent electrical circuit [7].

1.6.1 Butterworth-van Dyke equivalent circuit

Butterworth and van-Dyke showed that a mechanically vibrating system driven by means of an electromagnetic field could be presented as electrical circuit. Figure 9 represents the equivalent circuit of the QCM, which is known as the Butterworth-

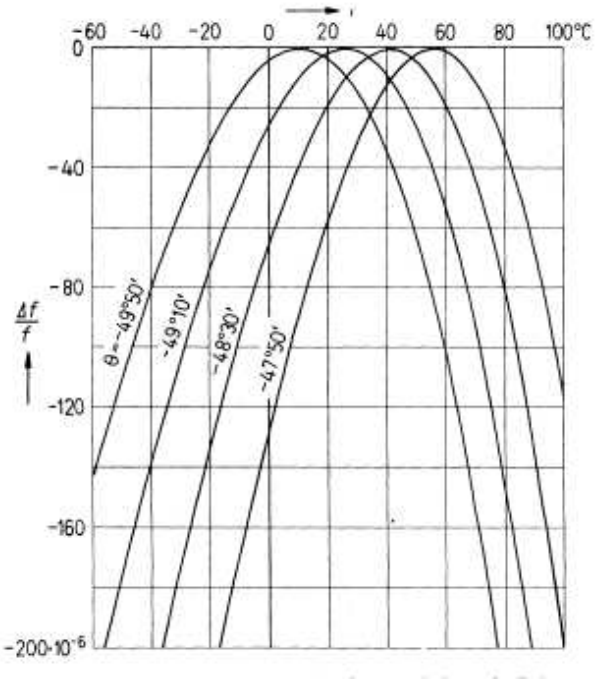

Figure 8. Frequency-temperature characteristics of BT-cut crystal [17].

van Dyke (BvD) equivalent circuit. In its simplest case the quartz plate can be approximated by a simple parallel-plate capacitor having a capacitance

$$C_0 = k\epsilon_0 \frac{A}{d}, \tag{9}$$

where A is the area of the electrodes, d is the thickness of the plate, k is the dielectric constant and ϵ_0 is the electric permittivity [11]. The motional capacitance

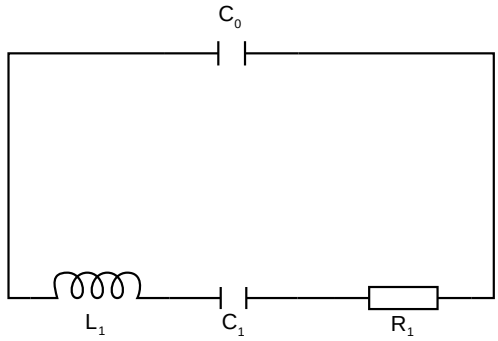

Figure 9. Butterworth-van Dyke equivalent circuit.

C_1 presents the mechanical elasticity of the vibrating body and the motional inductance L_1 is a measure of the vibrating mass. The resistance R_1 corresponds to losses of the crystal, which are due to internal friction and energy dissipated to supporting structures [7]. Near the resonance frequency these parameters get the following values

$$L_1 = \frac{d^2}{8C_0c^2v} \tag{10}$$

$$C_1 = \frac{8C_0c^2}{\pi^2n^2} \tag{11}$$

$$R_1 = \frac{\pi^2n^2\eta e}{8d^2A}, \tag{12}$$

where c is the coupling constant, η is the viscosity of quartz, n is the mode number and e is piezoelectric coefficient [10]. The Q factor of the circuit is

$$Q = \frac{1}{2\pi f_n R_1 C_1}. \tag{13}$$

Then using equation (5), (11) and (12) we get:

$$Q = \frac{d^2A}{\pi v\eta C_0c^2} \tag{14}$$

In QCM applications one has to add an extra capacitor C_L in parallel, which describes the load of mass deposited to the surface of the quartz. Equivalent circuits are seldom used, because components in the circuits are rather hard to determine exactly for the quartz crystal [10].

Quartz crystals have many advantages over conventional components in electrical circuits. These advantages are lying in the component values of the quartz crystal, which conventional components would have to provide in order to simulate the behavior of the quartz crystal. Typical 5 MHz AT-cut crystal would have a capacitance C of order 0.01 pF, which is impossible to replace by a conventional

electrical capacitor. The value of L is of the order 0.1 H and R = 10 Ω. A coil having such a large inductance require many turns of wire. Constructing such a coil with a resistance of only 10 Ω in such a small volume might be problematic [11].

1.7 Electrodes

To apply electical field on the quartz surface thin metal electrodes are needed. Also a final adjustment of the resonance frequency is made with the electrodes [11]. Electrode materials are usually applied by sputtering. The most commonly used metals are silver, gold and aluminium. Usually silver and gold are preferred to aluminium, because they are both chemically stable and do not form oxide layer like aluminium. However this chemical stability introduces problems to adhere on the surface of the quartz, thus a thin layer of chromium is often deposited on the quartz to improve adherence, because it forms a SiO_2-oxide-metal bond [11]. A disadvantage when using chromium is the increasing stress in the electrodes [8]. Stress tends to bend the crystal which will shift the resonance frequency [7]. Recently it has been found in ref. [18] that by replacing the conventional gold electrodes with porous gold electrodes the mass sensitivity of the QCM was enhanced by a factor of 40 without affecting the Q factor. This is because with porous electrodes the total surface area is increased, thus increasing the sensitivity. Usually the thickness of the electrodes of the quartz crystal used in microbalance application is 100 nm [19].

The electrodes are usually made key-hole shaped, thus making the resonator thicker in the center than at the rim. This focuses the displacement field to the center of the crystal by a mechanism called energy trapping [11]. Actually the optimal electrode shape for AT-cut quartz resonators is almost elliptical. A formula for the optimal shape was first derived by Mindlin [20].

1.8 Energy trapping

In a vibrating system resonance is associated with the phenomenon of standing waves. The theory of energy trapping is based on the principle that traveling waves can propagate and produce standing waves and resonances only for frequencies above a certain minimun value called the cutoff frequency. The cutoff frequency of the quartz crystal is the fundamental mode frequency [11].

Quartz resonators need supporting structure someway connected to its surface. To avoid any damping of oscillations the vibrations must be limited to a certain area, which is away from the physical contact points [7]. Electrodes adjusted on the plate of the quartz serve a boundary between the plated and unplated regions of the quartz. Due to smaller cutoff frequency of the plated area than the unplated area the standing acoustic waves cannot be formed beyond this boundary and energy trapping occurs [8].

Another way to introduce energy trapping is to make quartz with one or both sides with curved faces [8]. This has been proven to be the most effective for low resonance frequencies (less than 8 MHz) [10].

1.9 Mass loading

To use a vibrational system for determining the mass, few conditions have to be fullfilled:

-The vibrational system should be easily excited by means of electromagnetic field
-A frequency measuring device can be coupled to the vibrational system without significantly disturbing it
-The resonance curve of the vibrational system has to be sharp, the change of the resonance frequency due to the deposited mass must be larger than the instability of resonance frequency

-The resonance frequency changes due to environmental disturbances caused by temperature fluctuations or external stresses should be small [7].

The accuracy in the mass measurements depends on how accurately the resonance frequency of the quartz crystal can be determined. In comparison with other physical quantities such as velocity and temperature, frequency is the quantity which can be determined in the most accurate way. The international system (SI) of units for time and frequency are obtained in laboratories using very accurate atomic frequency standars called primary standars. Since time is inversely proportional to frequency it is easy to derive a frequency standard from a time standard and vice versa. Nowadays the most accurate frequency standard is obtained from the transition between two hyperfine levels of the ground state of the cesium atom 133. The radiation produced by the transition is exactly 9 192 631 770 Hz [21].

1.9.1 Small Mass Approximation derivation of Sauerbrey's equation

Sauerbrey's equation (3) was the first equation which related the frequency change linearly to the mass deposited on the QCM. In this subchapter the short derivation of this equation is presented. The effects of the electrodes of the QCM are ingnored.

For a quartz resonator to oscillate in the fundamental thickness-shear mode the following equation must be satisfied

$$d_q = \frac{\lambda_q}{2}, \tag{15}$$

where λ_q is the wavelength of shear-mode elastic wave. Since

$$\lambda_q f_q = v_q, \tag{16}$$

equation (15) reduces to

$$f_q d_q = v_q/2 \tag{17}$$

Assuming that the resonance frequency shift df_q is caused by an infinitesimal change in the crystal thickness dd_q. This can be written as

$$\frac{df_q}{f_q} = -\frac{dd_q}{d_q} \tag{18}$$

where the negative sign indicates that the increased mass decreases the resonance frequency. The increased thickness is associated with the increase of the quartz crystal mass M_q and then making assumption that for small mass change, the addition of foreign mass can be treated as an equivalent mass change of the quartz, (18) reduces to

$$\frac{df_q}{f_q} = -\frac{dM}{M_q}, \tag{19}$$

where dM is an infinitesimal amount of foreign mass. This mass can be expressed as M_f. The equation (19) gets form

$$\frac{(f_c - f_q)}{f_q} = -\frac{M_f}{M_q}, \tag{20}$$

If one then defines the areal densities m_f and m_q as the mass per unit area for the deposited film, then quartz crystal equation (20) can be written in the form of

$$\frac{(f_c - f_q)}{f_q} = -\frac{m_f}{m_q}, \tag{21}$$

The areal density is defined as a product of thickness and density. Substituting this and equation (17) to the equation (21) yields

$$m_f = -\frac{(f_c - f_q)\rho_q v_q}{2f_q^2} \tag{22}$$

Equation (22) reduces to equation (3) by substituting $(f_c - f_q)$ by Δf. The coefficient $\frac{2f_q^2}{\rho_q v_q}$ is called as the mass sensitivity of a QCM. For example a 5 MHz AT-cut quartz crystal can have mass sensitivity 5.65 MHz m^2/kg which means that the addtion of a material with areal density of 17.7 ng/cm^2 will cause a frequency shift of 1 Hz. The equation (22) is valid only in an ideal case when the mass is deposited into the center of the quartz [7].

1.9.2 Z-match method

Because the film is treated as a small increment of the crystal, Sauerbrey's equation only applies to systems in which the deposited mass has the same acoustic properties as the crystal and the frequency change is small ($\Delta f/f \leq 0.05$). At larger frequency changes one has to use so-called Z-match method, where the areal density of deposited material can be obtained from the following equation

$$m_f = (\frac{\rho_q v_q}{2\pi Z f_c} tan^{-1}[Ztan(\pi \frac{(f_q - f_c}{f_q})] \tag{23}$$

where Z is the ratio of the acoustic impedances

$$Z = \frac{Z_q}{Z_f} \tag{24}$$

and $Z_x = \rho_x v_x$ is the characteristic shear-mode acoustic impedance. Equation (23) reduces to the orginal Sayerbrey equation (3) with Z = 1 and for very small mass [7].

1.10 The sensitivity and accuracy of the mass measurement

Equation (22) shows that the mass sensitivity of the QCM is proportional to the square of the frequency of the quartz resonator. As a consequence the mass sensitivity increases when the resonance freqency increases. The mass-sensitive area of the QCM is located in the center of the resonator [13]. In an ideal quartz resonator the amplitude of the vibration is maximum at the center of the quartz and falls of exponentially outside the center [21]. Figure 10 shows the mass sensitivity Δf and vibration amplitude U along one of the quartz crystal diameters [13].

The minimum detectable mass depends on the frequency stability $\frac{\Delta f}{f}$ in addition to the mass sensitivity. It was shown in ref. [13] that the frequency stability can be as high as $\frac{\Delta f}{f} = 1.5 \times 10^{-9}$, which results in 1 pg/cm^2 for the minimum detectable mass. Comparing to the conventional balances such as torsion or spring balances

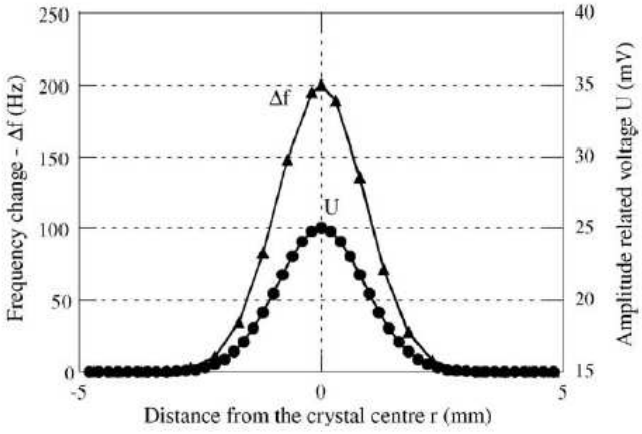

Figure 10. Mass sensitivity Δf and viration amplitude U as a function of the distance from the center of the crystal [13].

which have a minimum detectable mass in order of 1 μg, with QCM one can detect a million times smaller mass than with conventional balances [13].

Accuracy is by definition the degree of correctness of a quantity measurement. It is a measure of the deviation of the measurement results from its real value. In the context of accuracy a concept called reproducibility is usually introduced. Reproducibility is the ability of a single measurement to produce the same result each time it is done with same conditions. Quartz crystals exhibits a variety of instabilities which influece the accuracy of the mass measurment. In addition to temperature-influenced frequency deviations other instabilities can occur for instance aging and noise.

Aging effect is the systematic chance in the frequency which is caused by internal changes in the quartz crystal with time. The primary causes for crystal aging are stress relief in the mounting structure, changes in the crystals circuitry (usually caused by mass transfer) and possible changes in the crystal material. To achieve slow aging one should shield the quartz crystal hermetically in a vacuum.

Noise is the most important phenomenon which limits the accuracy of the quartz crystal. Noise in the quartz crystals is caused by short-term instabilities such as

temperature fluctuations and random vibrations. Other cause is the Johnson or white noise which originates from the charge carrier fluctuations. The Johnson noise is frequency independent but it is proportional to the bandwith. In the frequency domain the noise floor is limited by Johnsson noise which is at 290 K -174 dBm/Hz [21]. To get accurate measurements one has to try to achieve the largest signal to noise ratio. This can be achieved for instance by increasing the exitation power [21]. Alternative choice is to reduce the bandwith with special filters or to use signal averaging. The role of the Q factor for the accuracy and sensitivity is that with high Q factors the frequency change can be measured more accurately than with low Q factors.

1.11 Losses

Every acoustic wave propagating along the surface of a crystal has acoustic losses, which limit the maximum achievable Q factor. The intrinsic material Q-limit is defined as the product of Q×f, which depends on the material properties of the resonator [22]. The Q value of the quartz resonator is defined as the ratio of energy stored divided by the energy loss per cycle. Energy dissipation of the quartz resonator can be caused by, for instance, intrinsic acoustic losses, electrical losses which are depended on the conductivity and the thickness of the electrical material, losses due to mounting structure and acoustic losses due to atmospheric damping. The latter can be avoided by placing the crystal in vacuum [8].

At room temperature the intrinsic acoustic losses dominate. The dependency between the frequency of the resonator and the intrinsic acoustic losses can be represented with simple equation

$$\alpha(dB/\mu s) = 2.15f^2 + 0.45f \tag{25}$$

where α is the damping coefficient in dB/μs and f is in GHz [23].

The surfaces of the quartz crystals are usually polished in order to avoid losses due to surface irregularities [8].

1.12 Coupling

A quartz crystal without any connection to the measurement system is characterized by its unloaded quality factor Q_u. To use a quartz crystal it has to be connected to the measurement system, which entails a lowering of the Q [25]. The coupling in a quartz crystal may be either mechanical or electrical or a combination of both [11]. Due to coupling the Q factor is characterized by its radiation quality factor Q_r, which represents losses due to power which may be considered as leaving the quartz crystal and to be dissipated in the measurement system. The Q_u represents losses due to the crystal alone and the actual quality factor Q_l is given by

$$\frac{1}{Q_l} = \frac{1}{Q_r} + \frac{1}{Q_u} \tag{26}$$

The coupling parameter k is determined as the ratio of Q_u and Q_r. k can be also qualified as the square root of energy stored elastically divided by energy lost electrically [11]. The coupling parameter represents the efficiency with which energy stored in the quartz crystal is coupled to the external load and dissipated there. Sometimes the equivalent circuit of the quartz crystal is presented by a transformer with turns ratio n to describe the coupling between the measurement system and the quartz crystal [25]. Figure 11 presents an alternative form for the equivalent circuit of a quartz crystal. R_m describes losses due to mounting structure.

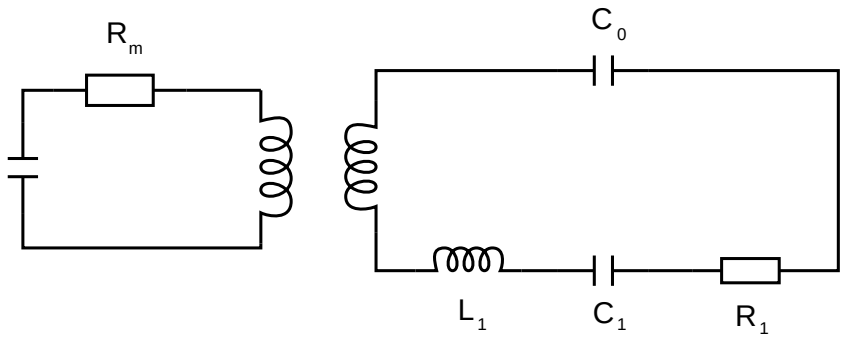

Figure 11. Equivalent circuit of QCM with coupling to measurement system [25].

1.13 Application for thin film deposition

There are many processes known for fabricating thin films such as evaporation, sputtering and pulsed laser deposition. If the density of the film is known the thickness can be calculated using mass measurement by QCM. The film growing applications usually require in situ measurement. The rate of the deposition is also a very important parameter to ensure that the film forms properly. A QCM offers simultaneous measurement of the thickness and the rate of deposition in situ even for ultrathin films whose thickness can vary from few molecular layers to several hundreds. [7].

As a disadvantage, the useful lifetime for the sensing crystal is limited and it has to be replaced with a new one because the accumulation of the film on the crystal reduces the sharpness and the quality of the resonance and the crystal can no longer sustain vibration. The Z-match method is commonly used in thin film applications due to acoustic mismatch especially if the film is thick. A disadvantage is that the ratio of the acoustic impedances has to be known. This ratio can differ in case of bulk material and in case of thin film. Many thin film processes need also the deposition of different materials. In this situation the mathematical analysis becomes rather complicated due to different acoustic impedances of different layers. A solution for multiple layers is to use multiple crystals [24].

As seen in previous subchapters the temperature and stress changes can shift the resonance frequency substantially. To ensure the accuracy of the rate of growth and thickness measurement in thin film deposition the so-called double resonance technique (DRT) is occasionally used. DRT consists of two quartz resonators with different cuts located close to each other so that the deposition will be the same for both crystals. With this arrangement temperature and stress effects can be eliminated [7].

2 Experiments with different quartz crystals at room temperature

The aim of the experiments with different quartz crystals at room temperature is to choose a proper crystal to operate as electron spin resonance (ESR) mirror in a Fabry-Perot cavity. This cavity is located in the sample cell of the commercial Oxford 2000 dilution refrigerator and it is used for studies of H in H_2.

2.1 QCM test setup

The experimental setup (fig.12) constructed for QCM studies at room temperature includes SR830 lock-in amplifier, HP8647A signal generator, directional coupler, RF detector and PC. The QCM is driven to resonance by means of RF power from the signal generator, which is coupled to QCM via a directional coupler. This type of measurement, where the changes of the reflection coefficient of the quartz crystal are measured is called the reflection method. In the measurements we used RF signal with the modulating frequency f_m. RF detector demodulates the frequency modulated signal and provides the voltage at the modulation frequency f_m proportional to the RF power. Lock-in amplifier uses phase-sensitive detection, in other words it rejects signal components which are not in phase with the reference. As a result with such frequency modulation technique we measure the derivative of the QCM resonance curve. Control of the equipment and recording of the DC signal from the lock-in amplifier is performed by a LabVIEW program. The program code and detailed operation of the program is described in the Appendix I. The PC is connected to the lock-in amplifier and to the signal generator through a GPIB (general purpose interface bus).

In addition to the measurement of the reflected signal from the QCM another possibility is to measure the transmitted signal through the crystal resonator. In

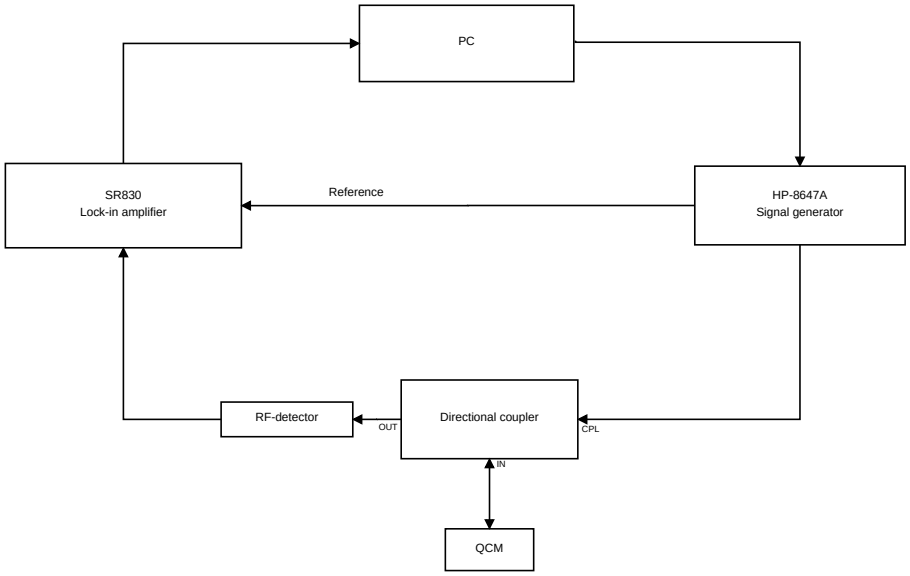

Figure 12. Schematic block diagram of the QCM detection system operating in reflection mode.

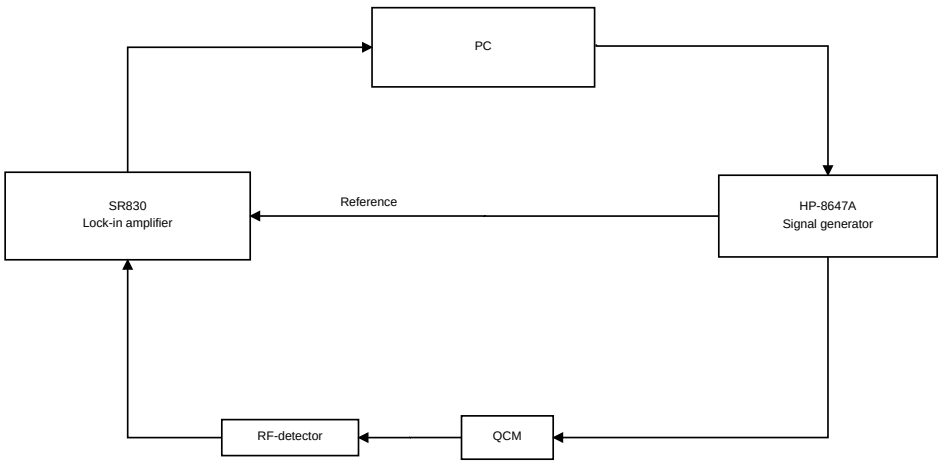

Figure 13. Schematic block diagram of the QCM detection system operating in transmission mode.

Table 1. The characteristic properties of different quartz crystals

Manufacturer	f_0 [MHz]	Diameter [mm]	Thickness [mm]	Cut
Morion Inc.	5	14.0	0.33	AT
Phonon	10	10.4	0.17	AT
ICM	10	8.0	0.18	AT
ICM	10	13.6	0.18	AT

transmission mode the quartz crystal is driven to resonance by means of RF power and the transmitted signal is detected by the Lock-in. The measurement system differs slightly from that for the reflection mode. The directional coupler is no more used. Figure 13 represents the measurement system in transmission mode.

2.2 Characteristic properties of different QCMs

QCMs from three manufacturer were tested in the experiments. Table 1 shows the characteristic properties of the different quartz crystals. Two of these crystal manufacturers Morion Inc [27] and International Crystal Manufacturing Co, Inc [19] produce commercial quartz crystals. Also non-commercial quartz crystals from LIT-Phonon institute (Russia) [28] were tested. In addition to bare crystals Morion and ICM provided also QCMs with electrodes. All crystals were AT cut. Morion crystals are not polished as well as ICM crystals. Only Phonon crystals are highly polished. In the ICM crystals electrodes are made in key-shape, unlike in Morion crystals which have different kind of electrode pattern represented in the figure 14. Electrodes of the Morion crystals are made of silver in addition to a small layer of chromium to improve the adhesion. The electrodes of the ICM crystals are made of gold and like Morion crystals they also have a small layer of chromium.

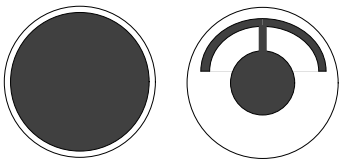

Figure 14. Electrode patterns of the Morion crystal.

2.3 Electrode manufacturing

Electrodes for LIT-Phonon and for some of Morion crystals were manufactured by sputtering a solid metal target. To provide a proper shape of the electrodes sputtering masks made of brass were designed. A reason for making electrodes ourselves was to avoid the chromium and the nickel layer used in Morion and ICM crystal. Quartz itself is diamagnetic, but the magnetic ordering of chromium in large magnetic field (4.6 T) may disturb the ESR measurements. Intead of chromium we deposited 15 nm thick layer of copper. Copper has full electron shells so it is only weakly diamagnetic. Balzers SCD 050 coat machine [26] has been used for sputtering.

2.3.1 The typical sputtering process

The thickness of the metal layer was estimated from the sputtering time versus sputtering current calibration curve from the operation manual [26]. First we sputtered a thin copper epi-layer to the quartz. For sputtering copper 40 mA current and 250 second sputtering time were used. After this the copper target was changed to the gold target. The gold is 99.9 % pure. For gold a sputtering current of 35 mA was used. A reason to use lower sputtering current for gold rather than for copper is that we noticed that the higher sputtering current leads to "island formations" on the surface of the quartz.

2.4 QCM supporting structures

The QCM has to be mounted onto some sample holder for measurement. A supporting stucture is also needed to make an electrical contact to the electrodes of the QCM [7]. The mounting has to be done in such a way that the stress to the quartz crystal is as low as possible. Electrical connection to the electrodes should be made near the edge of the crystal to avoid disturbing vibrations located at the center of the crystal.

One of the simplest ways to mount the quartz crystal and to make electrical connection to it is simply to glue wires to the electrodes. After that the QCM can be supported in the sample cell just with the wires. The reason why key-shaped electrodes are commonly preferred is that the gluing can be made close at the edge of the crystal. For gluing we used electrically conductive silver epoxy (Eccoshield VSM). A problem with gluing is to use a small enough amount of epoxy, so that it does not disturb crystal vibrations.

Another way to mount the crystal and to connect excitation leads is to do it mechanically. Mechanically made contacts have several advantages over gluing. The influence on the quartz vibration is less than that with gluing. Mechanical contacts also minimize the bending of the crystal. A disadvantage is that if the connection is made by pressing the metal against the electrode it easily scratches the electrode surface which may induce changes of the resonance frequency.

Figure 15 represents the mechanical supporting structure used for the room temperature measurement. The lower and upper part are made from POM plastic. Two rubber o-rings with copper wires are needed to provide the electrical contact to the QCM. This method was found to be the easiest and fastest way to mount the crystal for testing and replace them.

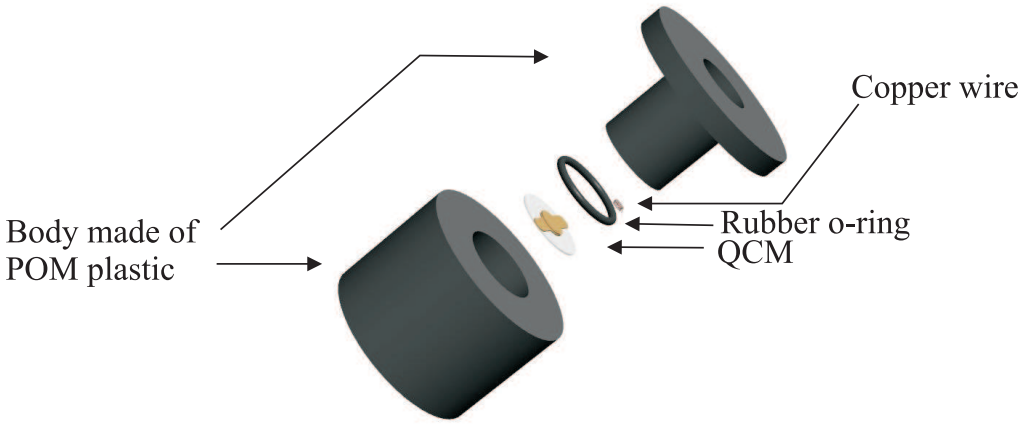

Figure 15. A schematic of QCM supporting structure.

2.5 Experiments

The typical experiment contains measurements of the resonance frequency, the width of the resonance curve Δ (measured as the Full width at half maximum (FWHM)), quality factor and the amplitude of the resonance curve for different quartz crystals. The influence of the thickness, size and shape of the electrodes to above mentioned parameters were studied. Figures 18 and 19 represent electrode shapes made for Phonon and Morion crystals. Also the difference between reflection and transmission methods was studied. To compare results, all measurements were made with same measurement parameters. RF power used for reflection measurements was -5.0 dBm which corresponds to 0.31 mW. With this excitation the signal to noise ratio is sufficiently high, which ensures high accuracy of the measurements. To make transmission measurements with the same RF power, the insertion loss of the directional coupler -20 dB was taken into account. Frequency modulation (FM) at $f_m = 78$ Hz was used. For both reflection and transmission methods the modulation amplitude was 100 Hz.

The resonance frequency is determined from the first derivative curve by taking the average of the minimum and maximum values of the frequency: f_0=(f_{max}+f_{min})/2.

The full-width-at-half-maximum Δ is determined from the peak-to-peak width: $\Delta f = f_{max}$-f_{min}. For Q factor calculations following equation can be used

$$Q = \frac{f_0}{\Delta f} \tag{27}$$

Typical first derivative curves of quartz crystal in reflection and transmission modes are shown in figure 16. Figure 17 shows original resonance curves for the same crystal obtained by numerical integration.

From the figures above it is clearly seen that the amplitude of the resonance in reflection mode is substantially higher than in transmission mode. This is due to mismatch of the impedances in transmission circuit. Also the width of the resonance curve Δf is more narrow in the reflection, which implies higher Q factors. A reason for lower Q factor is that the equivalent circuits in transmission and reflection are different. The transmission circuit has stronger coupling to the measurement circuit which consist of two separate coupling lines (compared to reflection, which has only one line shown in figure 11). Consequently the system loses power twice higher through these two coupling lines, which explains the lower Q factor [25]. Due to these results the reflection mode was chosen for further measurements. In table 2. results for quartz crystals are represented as a function of the electrode parameters: thickness, size, shape and material. Also the influence of the mounting structure is studied by comparing results taken with supporting structure shown in figure 15 and that of glued leads.

As a conclusion, the resonance frequency decreases as the electrode thickness increases, which is evident due to larger amount of mass to be vibrated. The amplitude of the resonance in Phonon crystals increased until thickness of 500 nm. Further increase of the electrode thickness did not result in any sizeable increase of the resonance amplitude. Morion crystal with electrodes prepared by the manufacturer showed the best resonance amplitude, which is probably due to large size of the crystal(smaller losses) and due to good adherance of the silver electrodes. This

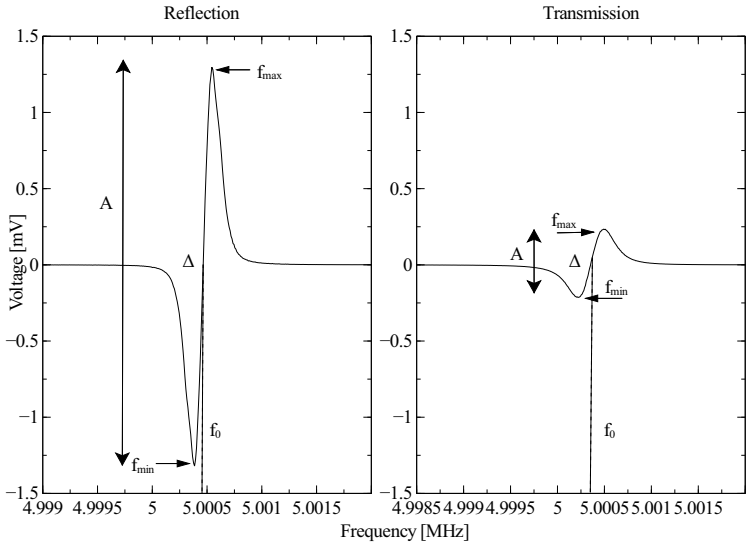

Figure 16. First derivate curves of the Morion crystal with silver electrodes in reflection and transmission mode.

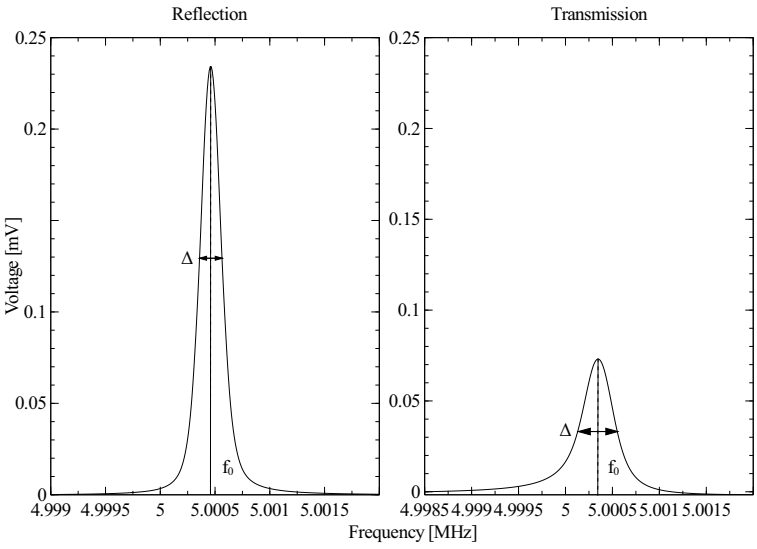

Figure 17. Absorption curves of the Morion crystal with silver electrodes in reflection and transmission mode.

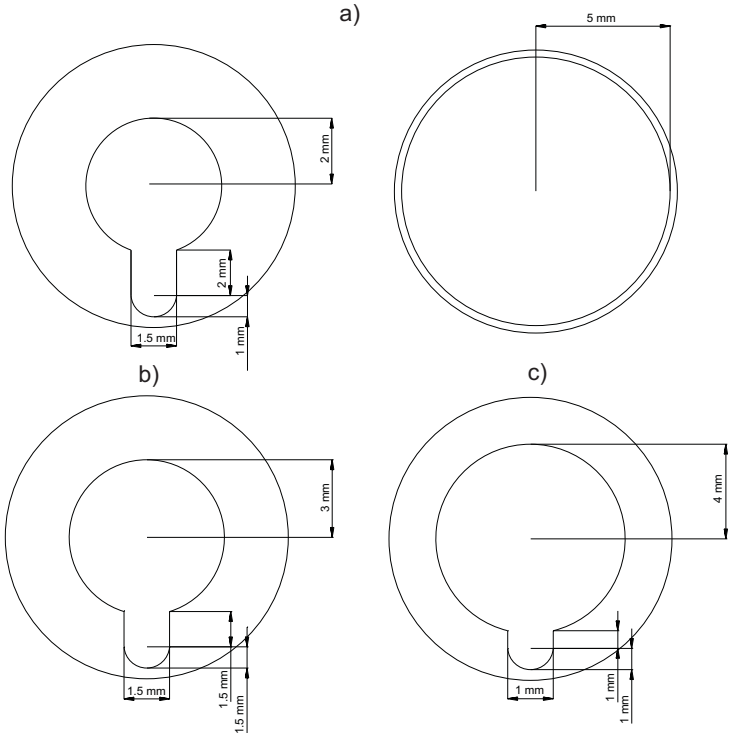

Figure 18. Electrode shapes of Phonon crystal

kind of amplitudes were not reached with homemade electrodes. This is probably due to impurities in the electrodes which cannot be totally avoided during the sputtering process. The highest Q factor was measured for Phonon crystal with 225 nm gold electrodes. Phonon crystals are highly polished which explains the highest quality factor. The difference between gluing and mechanical supporting structure was negligible, except for the large amount of glue., For example, Phonon crystal with 225 nm c) type electrode with glued leads resulted in large Δ and small quality factor.

We found that the reproducibility of the resonance frequency in air was rather poor. QCM may easily collect some dust, which may decrease the resonance frequency by several hertz. Aiming on measuring the resonance frequency more accurately one has to place QCM into a vacuum chamber.

Table 2. Results

Manufacturer	Electrode shape	Electrode thickness [nm]	Electrode material	Connection type	f_0 [MHz]	Δ [MHz]	Q	Amplitude [mV]
Morion		150	Silver	Mechanical	5.0005	0.000158	31670	2.8
Morion	e)	200	Gold(sputtered)	Mechanical	5.3946	0.000421	12812	0.72
Morion	d)	50	Gold(sputtered)	Mechanical	5.4605	0.001328	4111	0.0050
Morion	e)	100	Silver(sputtered)	Mechanical	5.4666	0.000326	16778	0.16
Phonon	a)	200	Gold(sputtered)	Mechanical	9.7469	0.000742	13206	0.40
Phonon	b)	225	Gold(sputtered)	Glued	10.2181	0.000261	39202	0.011
Phonon	c)	225	Gold(sputtered)	Glued [a]	9.7064	0.000631	1537	0.002
Phonon	a)	200	Gold(sputtered)	Mechanical	9.7463	0.000064	15615	0.52
Phonon	a)	500	Gold(sputtered)	Mechanical	9.5528	0.000462	20659	0.61
Phonon	a)	600	Gold(sputtered)	Glued	9.4181	0.000511	18421	0.58
ICM		100	Gold	Glued	9.9580	0.00102	9691	0.30
ICM		100	Gold	Glued	9.9626	0.000539	18489	0.52

[a] Large amount

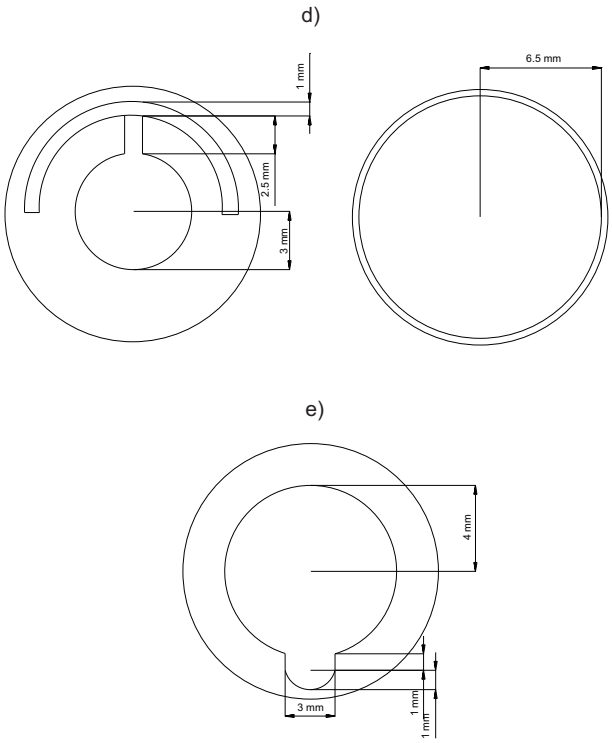

Figure 19. Electrode shapes of Morion crystal

2.5.1 The influence of the modulation frequency on the resonance curve

We found that the influence of the modulation frequency on the shape of the resonance curve was rather large. At higher modulation frequencies the width of the resonance curve increased showing lower quality factors. For different crystals the influence was different. For example, for Morion crystals the higher modulation frequencies (above 500 Hz) revealed double resonance peak structure in transmission mode, which disappeared when the modulation frequency was lowered. In the reflection mode the double peak structure was also seen but not so clearly as in the transmission, confirming that the equivalent circuits in transmission and reflection are not the same. For Phonon crystals such a stucture was seen neither in transmission nor in reflection, which implies that it is a characteristic property of Morion crystals. Different shape of the electrodes of the Morion crystals had negligible effect on the double peak structure. The reason for such a behavior can be found from the

spectrum of modulated signals. This spectrum consist of one carrier and several side bands. If the modulation frequency is higher than the width of the QCM resonance, the excitation contains several sidebands, which may produce several line instead of one and create complicated resonance lineshapes. Figures 20 and 21 represent the influence of the change of the modulation frequency for reflection and transmission.

2.5.2 Harmonic overtones

Measurement of the harmonic overtones was made with the Phonon crystal having 500 nm gold electrodes. The first harmonic is the fundamental frequency of the quartz here 9.5524 MHz, for the third harmonic $f_0 = 28.6319$ MHz, for the fifth $f_0 =$ 47.7508 MHz and so on. Figure 22 represents the first derivative curves of different harmonic overtones in reflection mode. As a conclusion peak-to-peak amplitude decreases as the mode number increases. This is due to losses at higher frequencies. It can also be verified that the harmonic numbers are not exactly odd numbers.

2.5.3 Q factor in different harmonic overtones

According to the equation (27) one could expect higher Q factors for higher harmonics. On the contrary equation (14) shows that the quality factor for higher harmonics should be lower. The reason for lower Q factors is the gain of intrinsic acoustic losses at higher frequencies according to equation (25). Figure 23 shows $1/Q$ values of different overtone modes from 1 to 13 at room temperature. The inverse quality factor is proportional to the losses of the crystal [29].

The curve shows a minimum for the 5th overtone. For higher overtones from 5th $1/Q$ is almost linearly proportional to the frequency, which implies that Q x $f =$ constant. Similar results were reported in ref.[29] at room temperatures. The mass sensitivity will increase at higher frequencies, but for the best Q value there exist an optimum (5th harmonic). At higher harmonics one will also get smaller signal

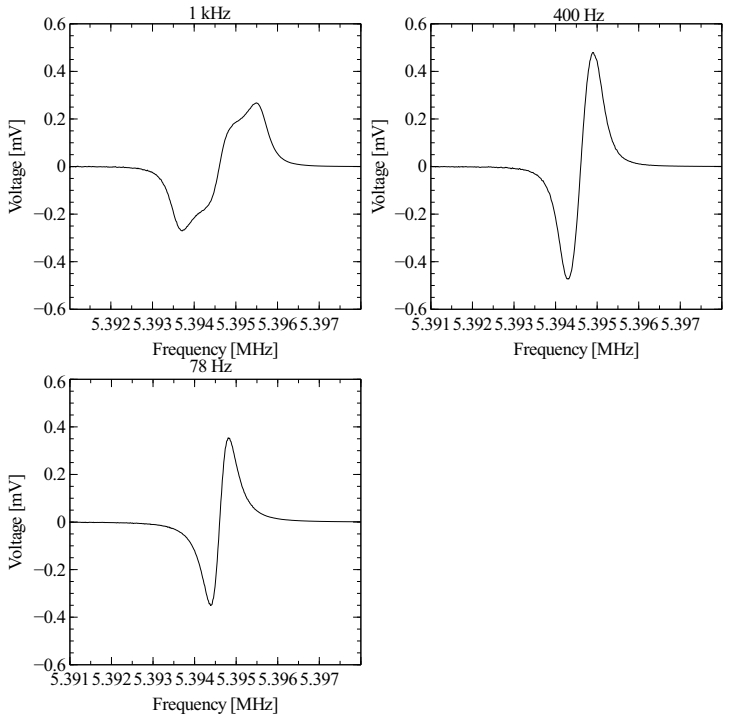

Figure 20. Influence of the modulation frequency to the reflection curve.

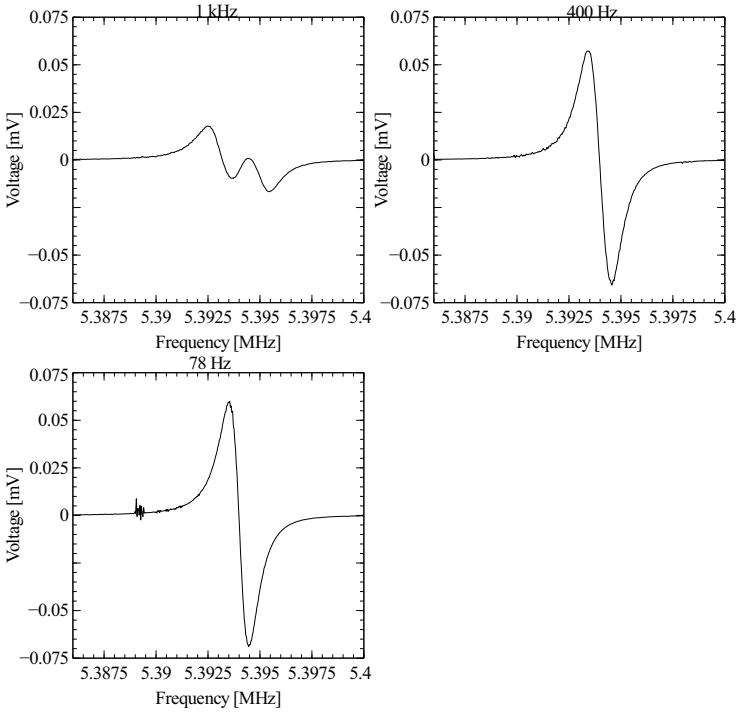

Figure 21. Influence of the modulation frequency to the transmission curve.

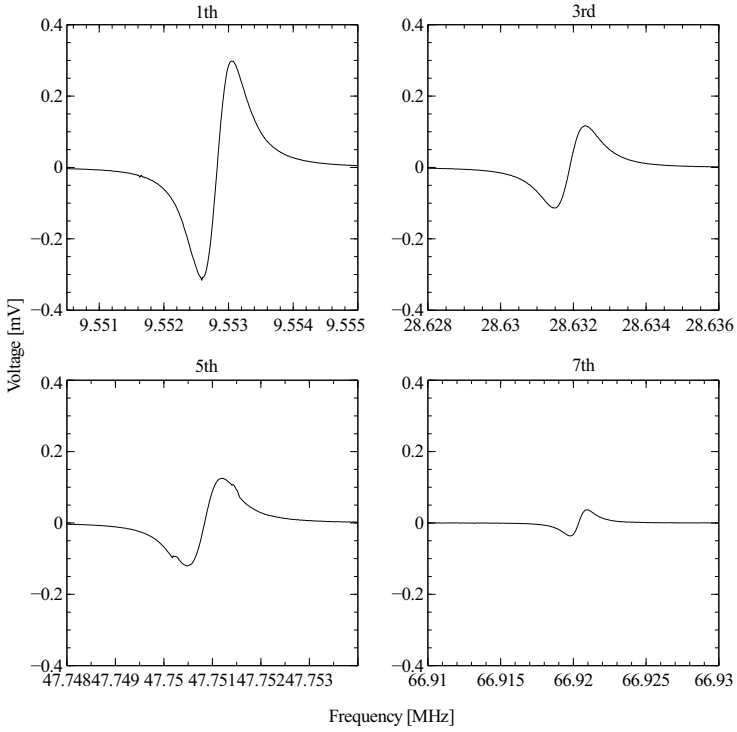

Figure 22. Harmonic overtones of the Phonon crystal with 500nm gold electrodes.

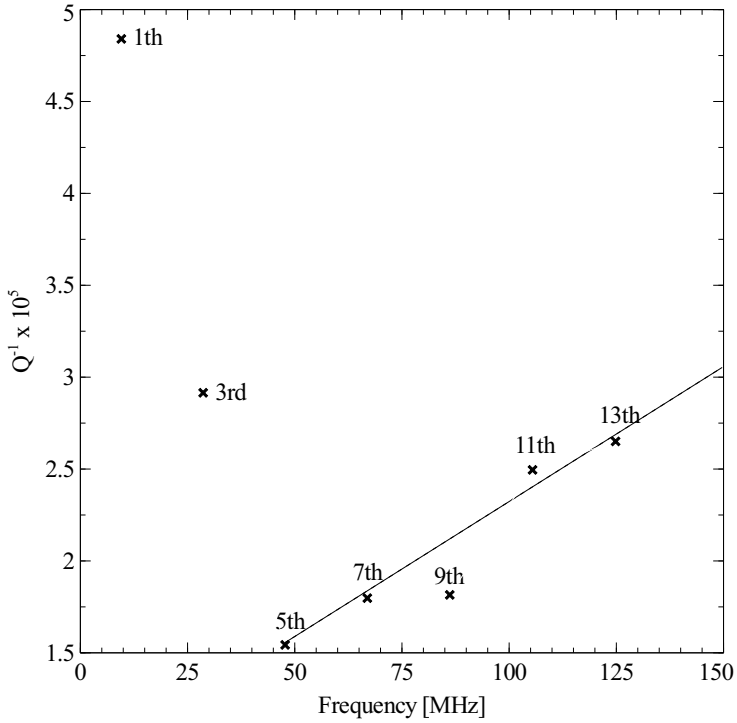

Figure 23. 1/Q for different overtones of the Phonon crystal with 500nm gold electrodes.

amplitude, which will create a detection problem at low excitation powers required at low temperatures. As conclusion one should use either 3rd or 5th harmonic to get the best sensitivity in the mass measurements.

2.6 Discussion

We have choosen to use Phonon crystal with 600 nm gold electrodes in the experimental setup at low temperatures. Phonon crystals have several advantages such as high quality of quartz and highly polished crystal surfaces. In that way they are the best choice to work as a mirror in the Fabry-Perot resonator. In addition of large Q factor it has large amplitude, which is an advantage for low temperature measurements. This is because the amplitude decreases linearly as a function of excitation and experiments at low temperatures usually require small excitation to avoid overheating.

3 QCM at low temperatures

QCM is an important tool in studies of gas desorption processes and friction in thin films at cryogenic temperatures. It has proved its power also in matrix-isolation spectroscopy [30]. Moreover QCM has been used in studies of quantum fluids like He^4 [3], [31], [32]. The first clear investigation of the onset of superfluidity in thin He^4 films adsorbed onto gold substrate was done with QCM. The superfluid transition can be observed as the increase of the resonance frequency, because unlike the normal fraction of a helium film the superfluid fraction does not remain rigidly coupled to the quartz motion [3]. The first complete characterization of the triple wetting transition of light molecular gases such as Argon (Ar), Krypton (Kr), Xenon (Xe), Nitrogen (N_2) and Oxygen (O_2) adsorbed on gold surfaces at low temperatures was done by the QCM [33]. Also more recently in ref.[34] wetting transitions of liquid hydrogen films on various substrates have been studied with QCM.

Due to the frequency-temperature characteristics it is important at low temperatures to ensure good thermal contact between the QCM and the cryogenic unit. This is because vibrations produce heat loads on the QCM, which may shift the resonance frequency [30].

At low temperatures the quality factor can be close to one million allowing measuring frequency changes more accurately than at room temperature [35]. The increase of the quality factor is due to a smaller amount of intrinsic acoustic losses. The decrease of the intrinsic acoustic losses at low temperatures follows a T^4 law. The losses are due to defects at the surface of the crystal, diffraction of the surface waves and due to energy losses through the supporting structure [23]. The acoustic losses are determined by the material characteristics of the quartz and they are independent of the cut of the crystal. It was shown in ref.[36] that there exists an acoustic loss peak at 5 K, which can be attributed to the two-level energy excitation process in which phonons are absorbed and are re-emitted after one recombination

time. Phonons interact with ultrasonic signals excited in the quartz crystal resulting in a dissipation of acoustic energy [36].

3.1 Experimental setup for studies of H in H_2 samples

The QCM is located in the sample cell (SC) constructed for studies of H in H_2. The same setup can be used as well for studies of superfluid transition in thin liquid ^{4}He films. The SC is cooled by the commercial Oxford 2000 dilution refrigerator, which is able to reach 6 mK temperature.

The QCM detection system used at low temperature measurements is similar to the figure 12. The measurement program for QCM data aquisition was made with LabVIEW. The purpose of the program is to operate as a feedback loop which keeps the RF oscillator frequency at the QCM resonance. The feedback loop is done by means of PID (proportional integrate derivative) algroritm, which is programmed to drive the signal detected by the lock-in amplifier to zero. A reason to use this kind of program structure is that the program used at room temperature measurements measures the whole resonance curve which takes a lot of time at low temperatures, because of the large Q factor. Also the accuracy is better in latter program, which is 1 Hz due to accuracy limit of the signal generator. Code of the measurement program and detailed description is represented in the Appendix II.

3.1.1 Sample Cell

Figure 24 represents the basic structures of the SC. The main parts of the SC are the body made of copper and three copper flanges (”top”, ”quartz” and ”bottom” flanges). To connect the QCM to the bottom flange a holder from Stycast 1266 epoxy was made. QCM was first glued to the holder with its edges. The QCM separates SC into two volumes. The volume above quartz will be used for actual experiment with H in H_2. The volume below the quartz disk (helium volume) can be

filled with superfuild helium. Thin copper leads were glued to the electrodes of the QCM with conducting silver epoxy (Eccoshield VSM). In the final step the holder with the quartz and the leads was glued to the bottom flange.

To provide efficient cooling of the quartz the SC is designed in such a way that the bottom side of the QCM can flushed by liquid helium. With this arrangement it is also possible to study superfluidity of helium. Helium is fed through small capillary to the helium volume. To measure the temperature of helium a ruthenium oxide thermometer was installed into helium volume with 50 μm diameter superconducting NbTi wires. Due to poor thermal conductivity they provide a good thermal insulation for the thermometer.

To build a solid molecular hydrogen layer to QCM a special H_2 source is connected to the top flange of the SC. In addition for ESR measurements the top flange of the SC includes the spherical mirror and the waveguide with its supports. Figure 25 represents the SC assembled to the dilution refrigerator. Atomic hydrogen is produced in a cryogenic dissociator [4].

3.1.2 Molecular hydrogen source

The main parts of the H_2 source are the body made of copper, beam tube and three steel tubes. Figure 26 represents the main parts of H_2 source source. The H_2 source is kept at 5 K since it is well insulated thermally from the sample cell via the stainless steel tubes. For coating the target surface cold molecular beam epitaxy is used. 5 K temperature is needed for obtaining H_2 molecules by sublimation from the solid phase. Due to the lower temperatures of the SC (below 1 K) molecules "freeze" to the target, which prevents clustering and provides uniform thickness of H_2 films [4].

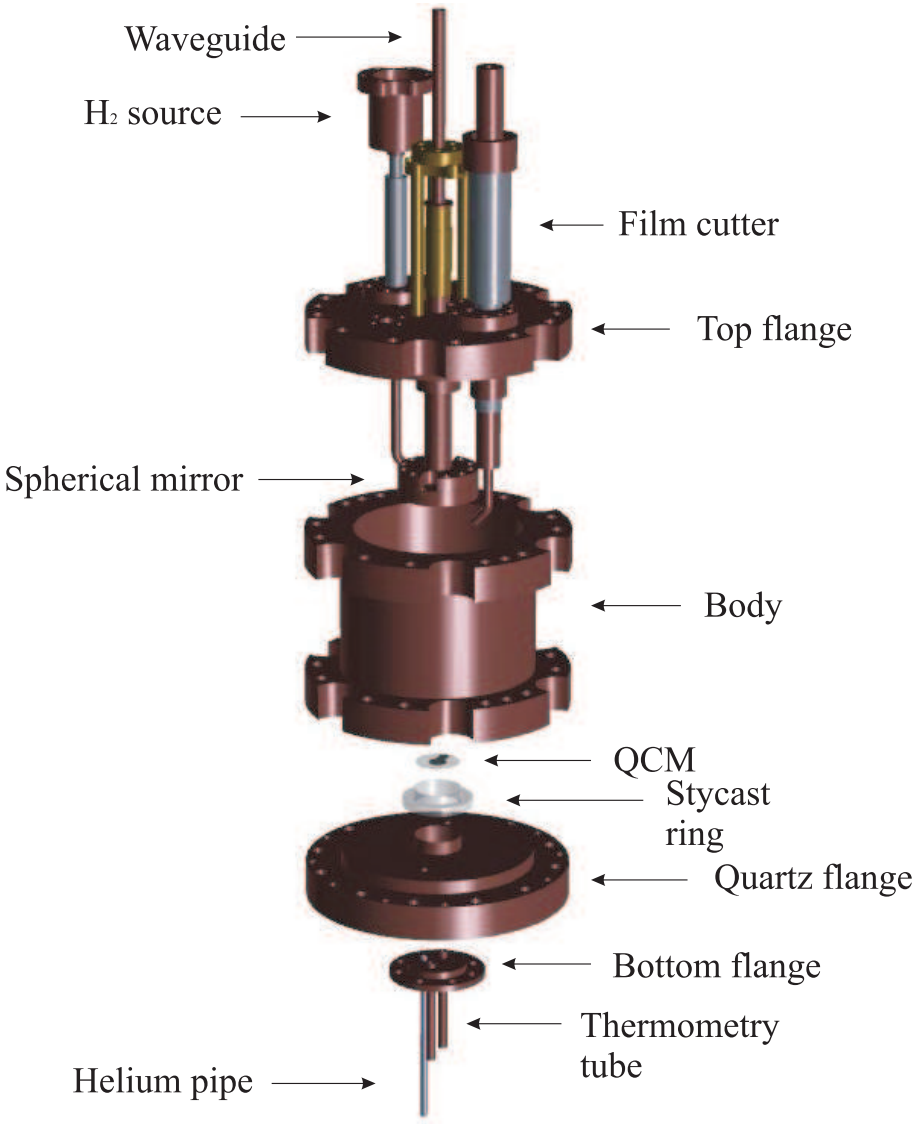

Figure 24. A schematic of the SC.

Figure 25. A schematic of experimental setup.

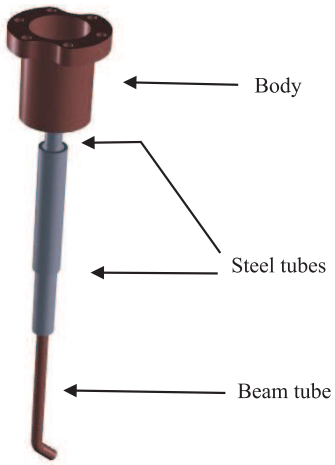

Figure 26. A schematic of molecular hydrogen source.

3.2 Experiments and results

3.2.1 Leak and cryogenic tests of QCM

To ensure that the SC is hermetic at cryogenic temperatures, the following leak test was made. The leak test consist of two parts. First stage is to ensure that the whole SC is hermetic. Second stage is to confirm that volumes inside the SC are leak tight with respect to each other. Figure 27 represents an arrangement used in leak test. Two different spaces of the SC and the space beneath the QCM were connected together with vacuum tubes to avoid large pressure difference. Leak test was made with Balzers QualyTest HLT 260 leak detector [37].

Some leaks may appear only at low temperatures, that's why the above mentioned leak test was done also at liquid nitrogen (LN_2) temperature by dipping the SC in to LN_2. Helium does not penetrate to SC parts embedded into LN_2 so SC can be leak tested by slowly lifting it from the LN_2 bath and blowing helium to the SC parts. At LN_2 temperature resonance frequency of the quartz dropped to 9.416766 MHz which is due to frequency-temperature characteristic of the AT-cut quartz.

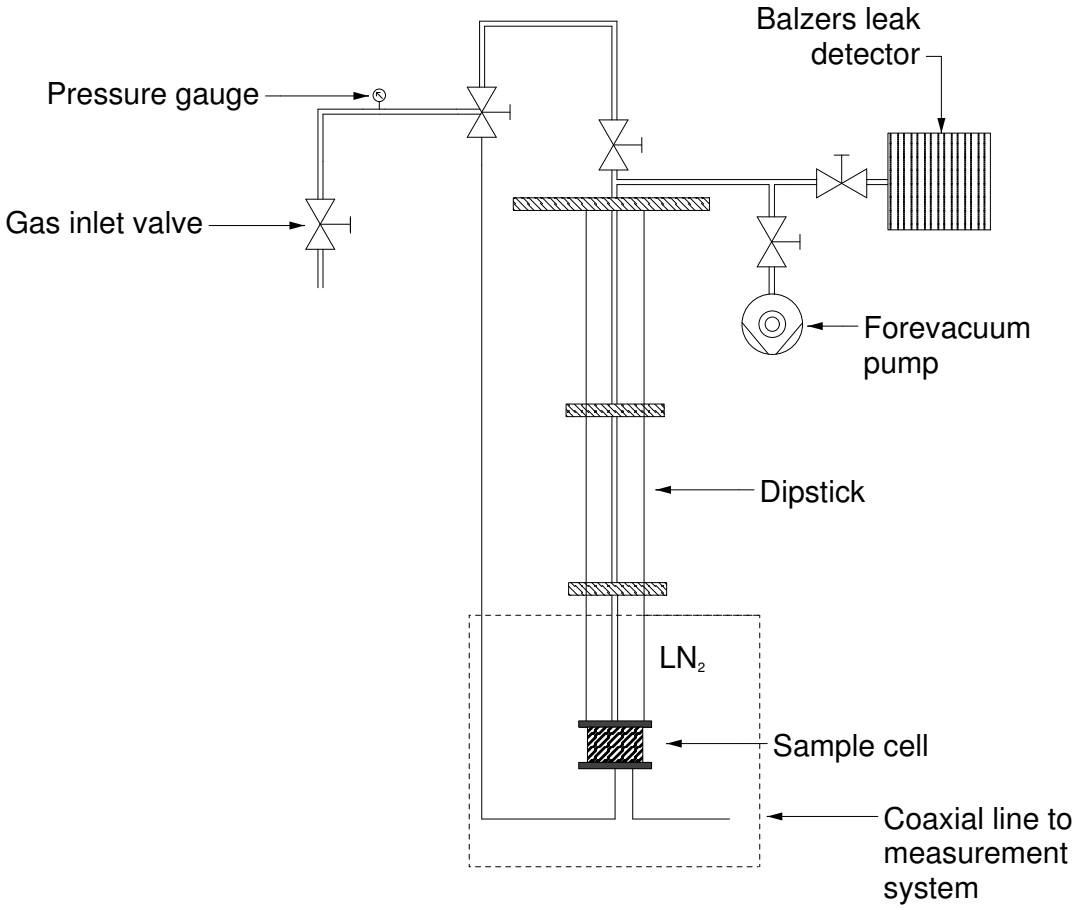

Figure 27. A schematic of the leak test arrangement.

Leak test of the sample cell with respect to the helium volume was done at LN_2 temperature by releasing 20 mbars of helium into the quartz volume. No leaks were found at such pressure difference.

3.2.2 Stability of the QCMs resonance frequency

The stability of the quartz was tested at LN_2 temperature at -25 dBm excitation. This was done by immersing SC into a dewar of LN_2 and letting a turbopump to maintain vacuum inside the SC. Figure 28 represents the change of the resonance frequency as a function of time.

We found that the resonance frequency stability tested by the setup represented

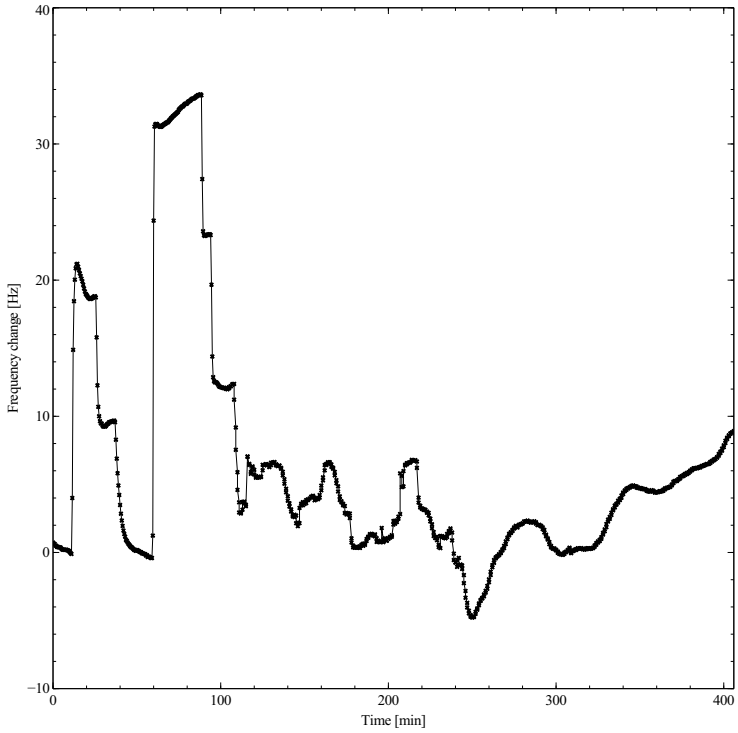

Figure 28. Stability of the resonance frequency at LN_2 temperature

in figure 27 was strongly dependend on the amount of LN_2 in the dewar. This is evident due to frequency-temperature characteristics of the coaxial lines connecting quartz to the room temperature device. The steps represents moments when the amount of LN_2 was added to dewar.

Because the observation of the supersolid behaviour of H_2 or H in H_2 requires detecting very small changes of the QCM resonance frequency, the frequency stability is important. The stability of the quartz was tested at 100 mK temperature at -40 dBm excitation in the dilution refrigerator. Figure 29 shows the change of the resonance frequency as a function of time.

In addition to the long term stability a short term stability was measured at 100 mk temperature at -40 dBm excitation. Figure 30 represents the short term stability.

The mean deviation (RMS) calculated from the average and frequency drift is

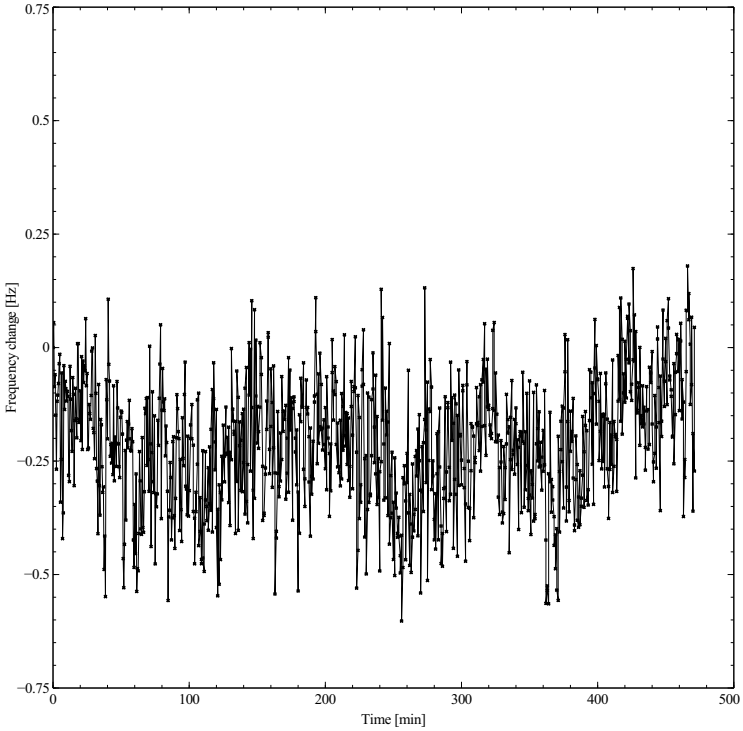

Figure 29. Long term stability of the resonance frequency at 100 mK temperature

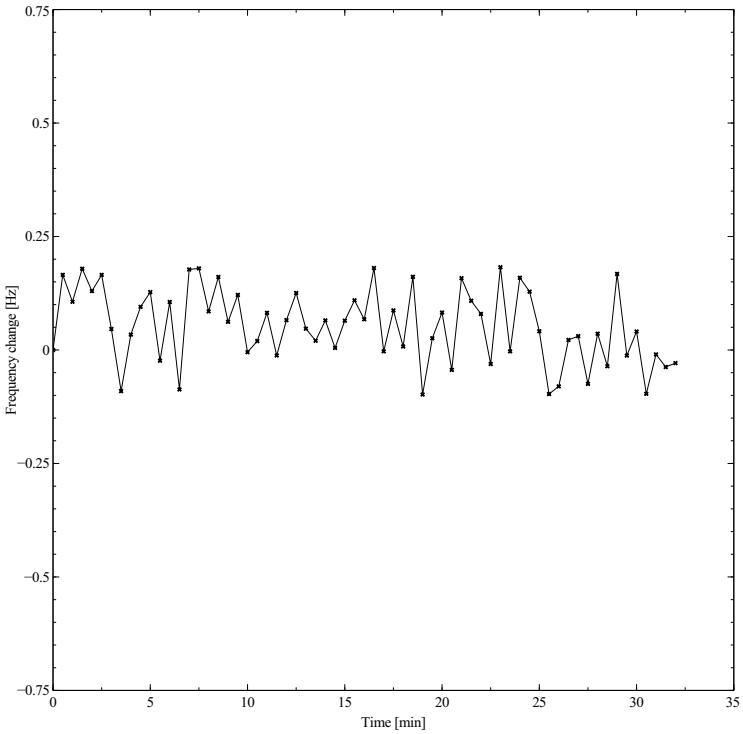

Figure 30. Short term stability of the resonance frequency at 100 mK temperature

0.3 Hz in long term and 0.1 Hz in short term. These are needed for the estimation of the minimum mass decoupling, which can be detected. With this stability our QCM is capable of detecting 1 pg/cm^2 mass changes.

3.2.3 Response to pressure differences

The response of the quartz to pressure differences was tested by letting nitrogen gas to the quartz volume and to the SC body. Figure 31 represents the change of the resonance frequency as a function of time at room temperature, when nitrogen gas was released to the SC body. As a result the frequency change is almost linear to the pressure change, which implies that quartz crystals can be used as in situ pressure gauges. We found that the frequency change had different sign when nitrogen was pumped to the quartz volume. This is due to different sign of force which bends the quartz crystal. Figure 32 shows the influence of the pressure to the resonance frequency at LN_2 temperature, when helium gas was admitted to the quartz volume. The frequency shift at LN_2 temperature is approximately 2.5 times larger compared with that for room temperature due to increase of gas density at low temperatures.

3.2.4 Temperature dependence of the QCM resonance frequency

Knowledge of temperature dependence of the QCM resonance frequency with the empty sample cell is important to account for this effect in the real experiments with hydrogen samples. Figures 33 and 34 represents the temperature dependency at -40 dBm and at -55 dBm excitation. We found that the frequency was temperature independent below 0.2 K. At higher temperatures the frequency change was almost linear.

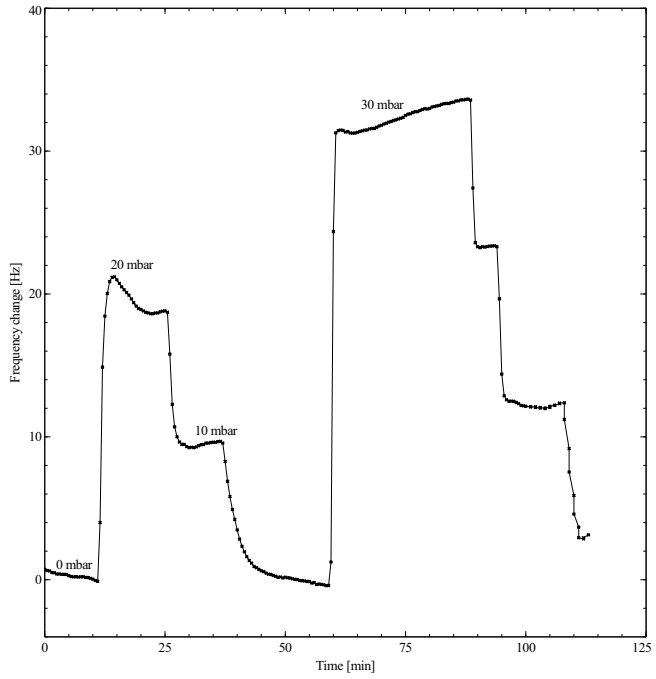

Figure 31. The influence of the pressure on the resonance frequency at room temperature

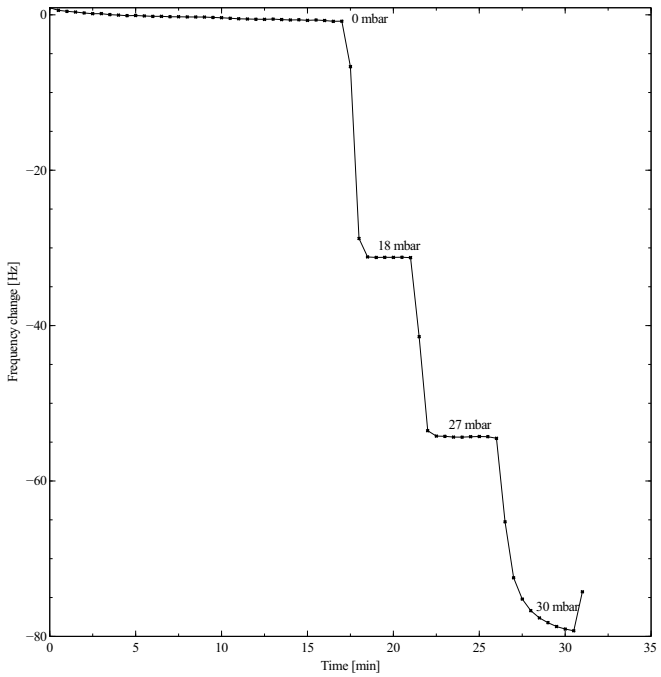

Figure 32. The influence of the pressure on the resonance frequency at LN_2 temperature

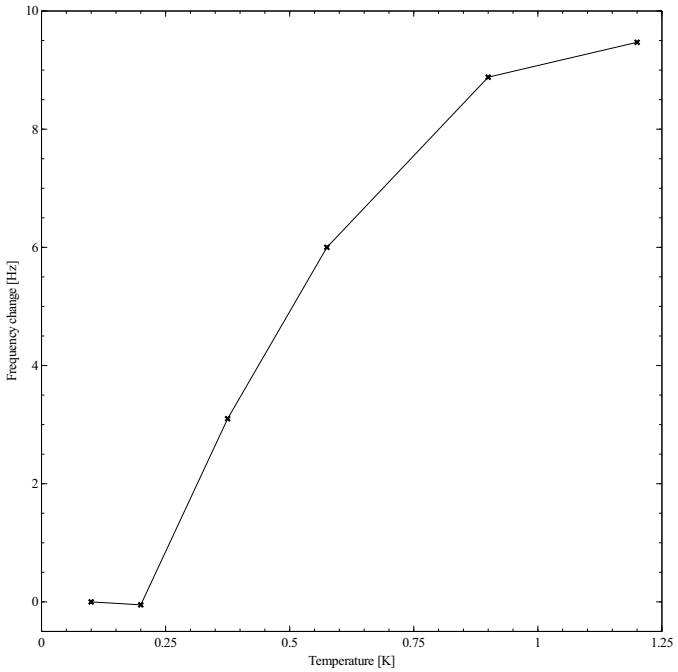

Figure 33. Temperature dependence of the resonance frequency at -40 dBm excitation

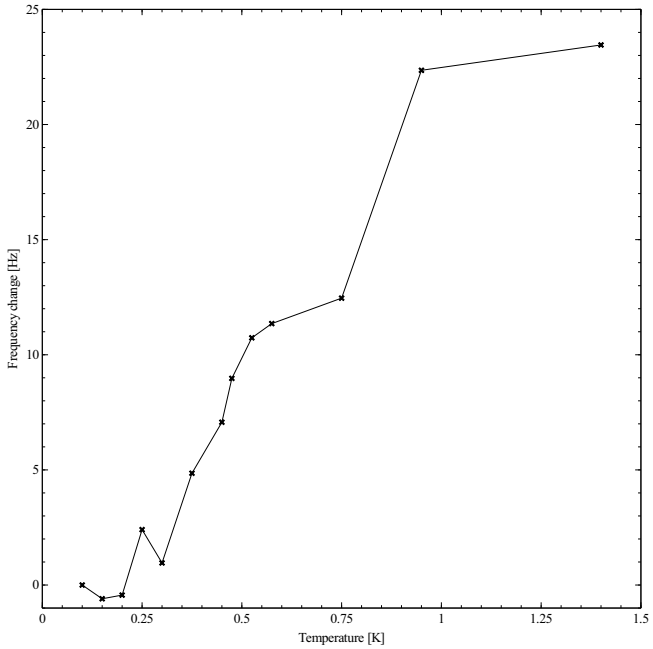

Figure 34. Temperature dependence of the resonance frequency at -55 dBm excitation

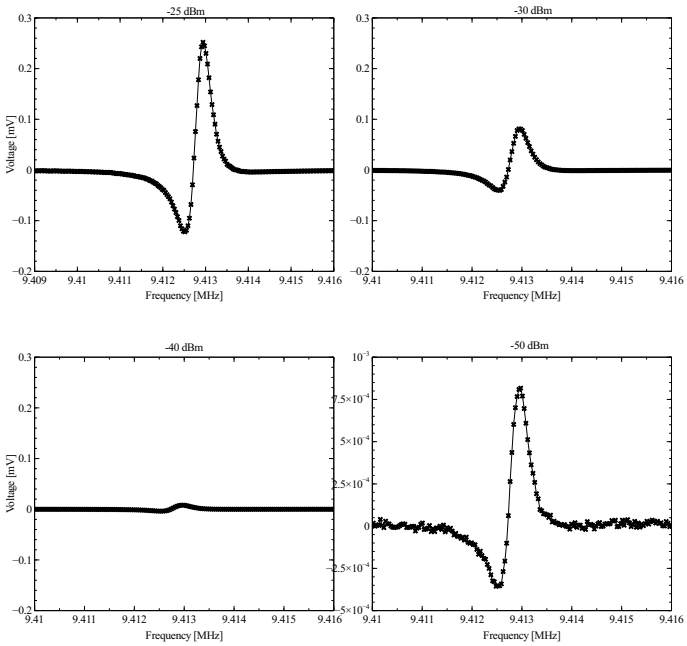

Figure 35. Derivative curves at 1 K at different excitation

3.2.5 Q value at cryogenic temperature

Derivative curves presented at Figure 35 were measured at 1 K temperature at several values of excitation, ranging from -25 dBm to -50 dBm. The Q value obtained from the derivative curve was 23532. The vibration amplitude enhanced by 0.17 mV (by a factor of 1.4) from the room temperature value which is evident due to reduction of losses in the connecting cables.

3.2.6 Harmonic overtones

Harmonic overtones were measured at 1 K temperature several values of the the excitation power. Figure 36 represents the 3rd harmonic curves at excitations ranging from -20 dBm to -50 dBm. Figure 37 represents the 5th harmonic curve at -40 dBm exctitation. The 3rd harmonic is resonating at 28.2312 MHz and the 5th harmonic is resonating at 47.1292 MHz. Q value for 3rd harmonic is 28340 and for 5th harmonic 47129. As concluded in chapter 2.5.3 one should take 3rd or 5th harmonic to get

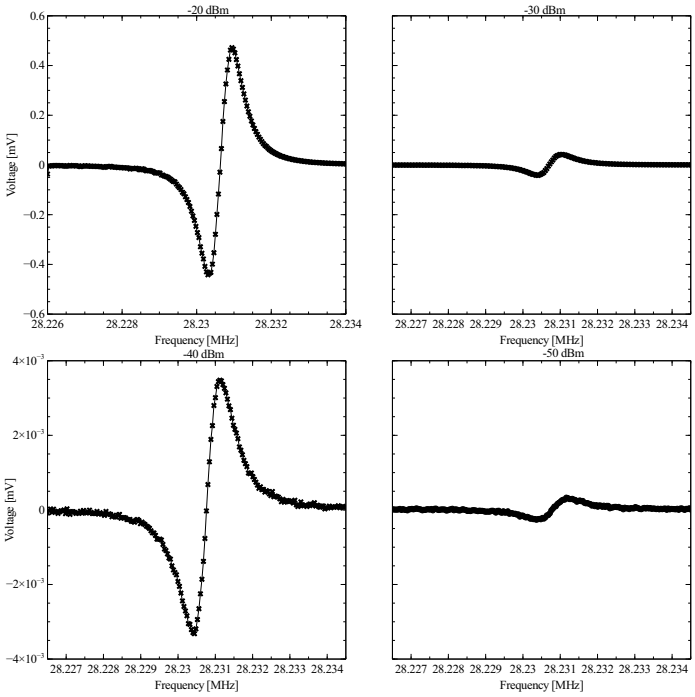

Figure 36. 3rd harmonic overtones at 1 K at different excitation

the best sensitivity in mass measurements.

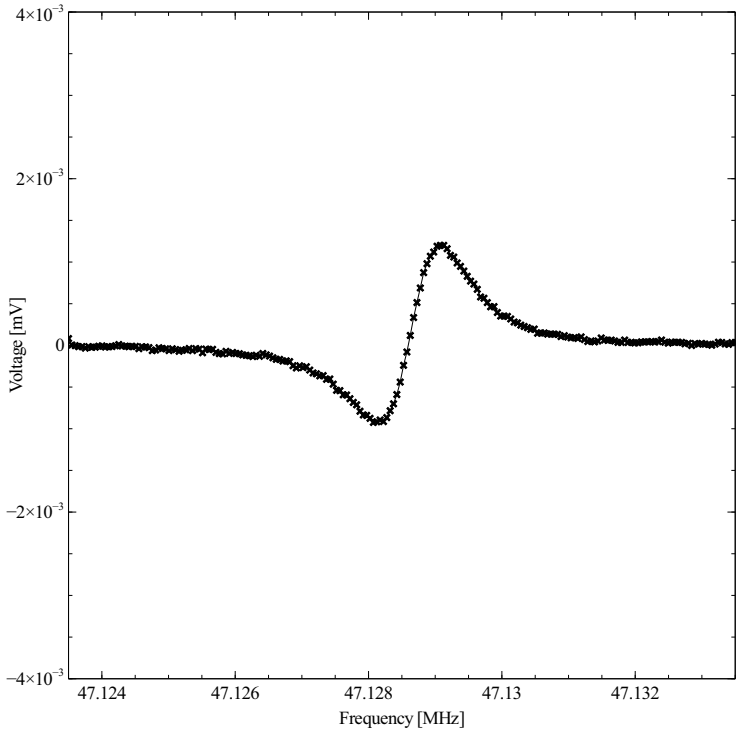

Figure 37. 5th harmonic overtone at 1 K at -40 dBm excitation

3.2.7 Approximation of the velocity of the vibration

To study superfluidity in helium one has to take into account that the velocity of vibration of QCM does not exceed the Landau critical velocity. In addition to detect supersolid behaviour of H in H_2 this condition has to be also taken into account. The critical velocity in this case is unfortunately unknown but it can be compared to critical velocity of thin helium films. Equation (4) describes the displacement in thickness-shear mode, which can be simplified to

$$u = A\sin(\omega t), \tag{28}$$

where $\omega = 2\pi$f. The velocity of vibration in thickness-shear mode is simply the derivative of the displacement, hence

$$u' = A\omega\cos(\omega t), \tag{29}$$

which gets its maximum value when cos(ωt) equals to unity. To calculate this velocity one has to know the vibration amplitude. According to ref.([13]) the vibration amplitude can be calculated from the equation

$$A = CQV, \tag{30}$$

where C = 1.4×10^{-12} m/V and V is the peak voltage applied on the quartz electrodes. From equations (29) and (30) it is evident that one should lower the excitation voltage as much as possible. However with very low excitation voltages the signal to noise ratio gets very small. At the excitation of -25 dBm the voltage at QCM electrodes is 12.8 mV. With Q values of 20 000 this corresponds the vibration amplitude of 3.58 Å. Then corresponding velocity of vibration at 10 MHz is 2.25 cm/s. Respectively at -40 dBm and with Q values of 20 000, the vibration amplitude is 0.313 Å and the velocity of vibration is 0.19 cm/s. Because the vibration amplitude gets its maximum at the center of the quartz also the velocity of vibration gets its maximum there. Velocity distribution across the QCM surface has a same shape of profile as shown in figure 10.

3.2.8 Future prospects for detecting supersolid behaviour of H_2 and H in H_2

A future application of QCM at low temperatures would be the observation of supersolid behavior of H in solid H_2. This exotic phenomenon is already observed in solid ^{4}He by Kim and Chan in 2004 [38] with a torsional oscillator. Similar theoretical predictions have been done for atomic hydrogen captured in the molecular hydrogen matrix [39]. Compared to helium, hydrogen does not need high pressure for solidification, however the difficulty to raise the H consentration in a H_2 matrix has been one of the major obstacles observing this exotic phenomenon. Also the observation of supersolid behavior of H would need very accurate measurements for which quartz microbalances serve a powerful tool. Similar to superfluid helium only

a small fraction of film may become superfluid at the transition.

The shift caused by one supersolid layer of H_2 in the resonance can be estimated by using the equation (22). In ref.[35] $\rho_q v_q$ is 8.862×10^6 kg/m^2 at cryogenic temperatures. Monolayer mass per unit area can be calculated using the surface density of hydrogen [4].

$$\frac{m_{mono}}{A} = m_H \sigma_H, \tag{31}$$

where σ_H is the surface density and m_H is hydrogen mass. The surface density obtained from the mean distance between atoms (3.3 Å) is 9.2×10^{18} atoms/m^2. Substituting values to equation 22 yields 0.61 Hz/H_2 monolayer deposited only to one side of the QCM. From this and from the stability measure for long an short (chapter 3.2.2) of the QCM frequency me we can estimate the minimum detectable mass decoupling. This provides an estimate of how large fraction of superfluid component we can detect. The maximum thickness of H_2 layer when QCM is still working in the linear mode ($\Delta f/f \leq 0.05$) is 250 μm. For this film thickness the detectable fraction of superfluid component is $\frac{\Delta m}{m}$ $\approx 6.60\times10^{-7}$ in long term and $\frac{\Delta m}{m}$ $\approx 2.20\times10^{-7}$ in short term.

3.2.9 Experiment with solid H_2

First we loaded normal H_2 to the H_2 source. This has been done by heating the filling capillary to high enough temperature, so that H_2 did not freeze anywhere else, but just in the H_2 source. Amount of H_2 condensed there was controlled by the frequency change of miniature RF resonator placed inside. We detected 1.5 MHz frequency change due to loading of H_2. Then the H_2 source was slowly warmed up with the SC temperature kept as cold as possible. Reaching 5 K at the H_2 source the H_2 started to move from the source to the top of the quartz. When the H_2 source was heated to 6 K the condensing rate increased significantly.

The SC temperature was hard to stabilize because of too strong thermal link of

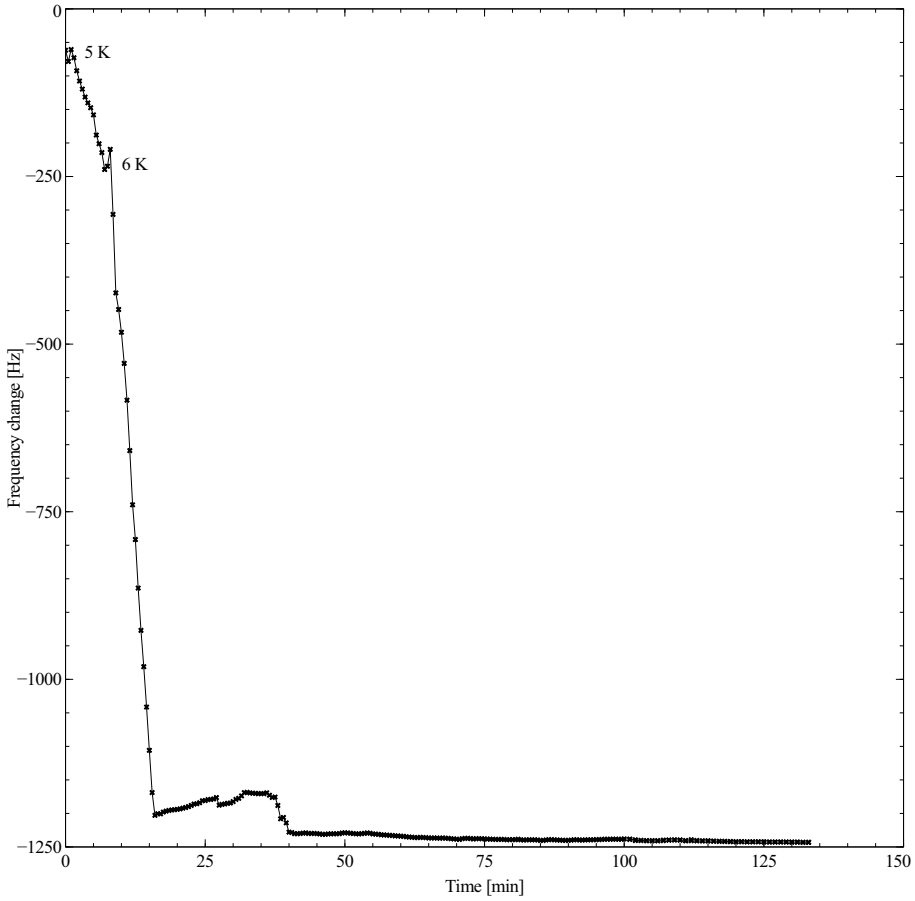

Figure 38. The resonance frequency shift due to H_2 condensed to the quartz

the H_2 source with the dilution refrigerator 0.1 K plate. These temperature drifts of the SC influenced the resonance frequency of the QCM. After heating the H_2 was stopped the SC was let to cool down to its minimum temperature. Figure 38 shows the resonance frequency shift due to H_2 condensed to the quartz. After condensing the resonance frequency remained stable which proved that the H_2 layer has frozen to the top of the quartz. The frequency shift is approximately 1100 Hz which corresponds to 0.55 μm thickness of H_2 film. For this film thickness the detectable fraction of superfluid component is $\frac{\Delta m}{m} \approx 3.00 \times 10^{-4}$ in long term and $\frac{\Delta m}{m} \approx 10 \times 10^{-4}$ in short term. For H in H_2 with a concentration of 0.1 % of H in 0.55μm layer H_2 the minimum mass decoupling is $\frac{\Delta m}{m} \approx 0.17$ in long term and $\frac{\Delta m}{m} \approx 0.06$ in short term.

4 Conclusions

This work demonstrates possible applications of quartz crystal microbalances in low temperature physics. In addition the thesis included basic information on the quartz resonators and their applications for mass measurements in thin films. The thesis contains detailed information of electrode manufacturing for bare crystals. The thesis gives also a good technical detail on the equipments needed to measure the resonance properties of the quartz crystals.

We studied properties of QCMs from three different manufacturers: LIT-Phonon, Morion and ICM. For two manufacturers: LIT-Phonon and Morion we manufactured electrodes ourselves using sputtering method. The influence of the thickness, size and shape of electrodes on resonance properties were studied. We analyzed the difference between transmission mode and reflection modes of the QCM detection. The highest Q values (39202) were measured for LIT-Phonon crystals with homemade electrodes. LIT-Phonon crystals are highly polished so they have smaller intrinsic losses. The highest resonance amplitude were measured with commercial Morion crystal.

Cryogenic tests of the QCM performance were done in real sample cell mounted inside the dilution refrigerator. We reached 0.3 Hz (RMS) long term and 0.1 Hz (RMS) short term stability of the QCM frequency measured with the excitation power of -40 dBm. Our QCM is capable of detecting 1 pg/cm^2 mass changes, this corresponds to the sensitivity of 0.03 % for the detection of possible mass decoupling in experiments on searching supersolid behavior in 0.55 μm thick H_2 films. We estimated that if atomic hydrogen impurity in the solid H_2 crystals would undergo supersolid transition in 0.55 μm thick films with 0.1 % concentration of atoms we would be able to detect superfluid fraction of 0.06. The maximum thickness of H_2 layer when QCM is still working in the linear mode was estimated to be 250 μm. For this film thickness we would be able to detect H_2 superfluid fraction of 2.20×10^{-7}.

We also estimated the velocity of the vibrations for QCM with the excitation power of -40 dBm. This corresponds to about 2 mm/s velocity of the QCM surface. Unfortunately critical velocity is not known for hydrogen, but it could be of the order of several mm/s, same as the critical velocity of helium films. In experiments we managed to condense H_2 to the surface of the quartz causing 1100 Hz shift to the QCMs resonance frequency. The shift corresponds to 0.55 μm layer of H_2. Next step will be to embed H atoms inside these films and search for possible superfluid behavior.

Appendix I

The function of the program is to record the derivative curve of the quartz. Program includes three input parameters: start frequency, stop frequency and number of points. Number of points determines the accuracy of the measurement. A subroutine based on linear interpolation is used to determine frequencies between measurement points. Figure 39 represents a flow chart of the program. First program writes new frequency value to HP 8647A and waits for 500 ms to make sure that the Lock-in amplifiers value is stabilized. After that program reads value from the Lock-in amplifier. Values are plotted and saved to a hard drive. In addition program calculates the resonance curve of the quartz by integrating the derivative curve. From the derivative curve program determines f_0, Δ, Q and the resonance amplitude.

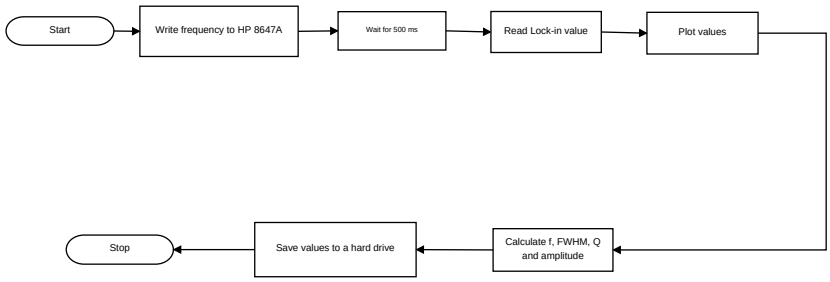

Figure 39. A flow chart of the QCM program

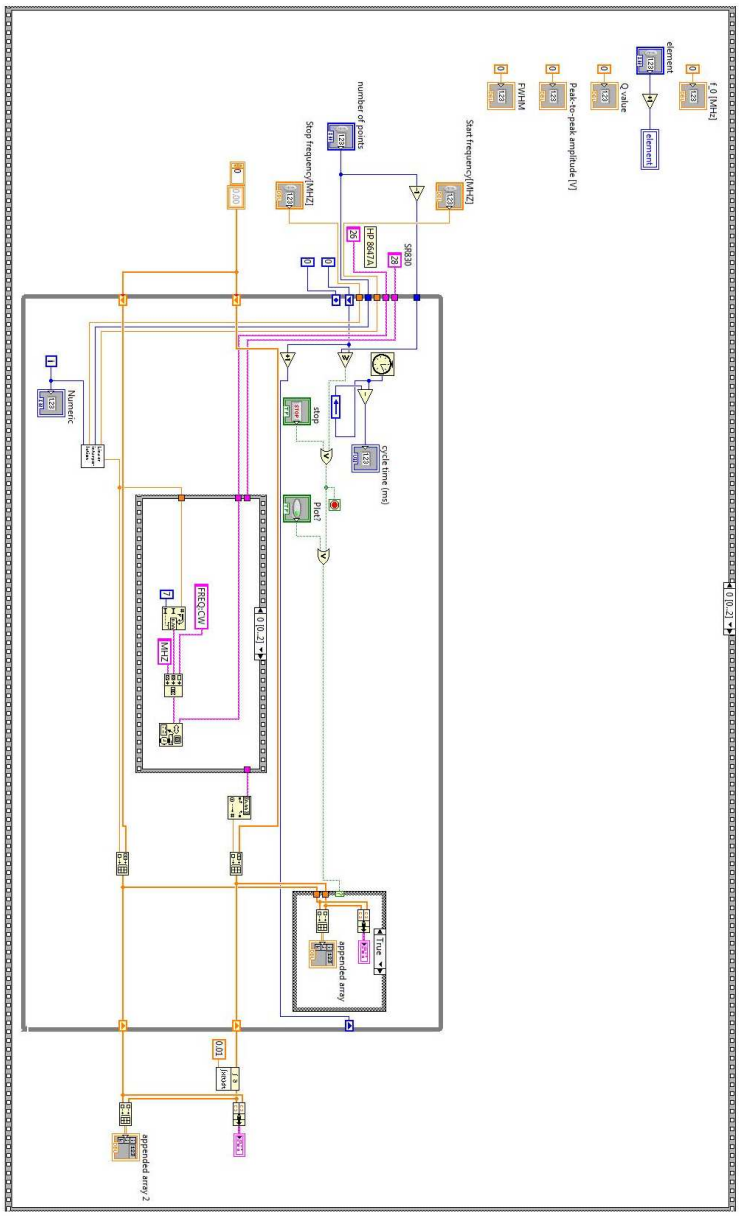

Figure 40. QCM program part 1

Appendix II

The main function of the program is to operate as a feedback loop to keep the quartz crystal at resonance. This is done by means of PID (proportional-integral-derivative) algorithm. The main idea in the PID is that it calculates a difference between a measured variable and a desired set point.

PID consist of three main values, which are called as proportional, integral, and derivative term. The sum of these variables is used to manipulate the variable. **Proportional term**: The proportional term depends only on the difference between the set point and the process value. Incresing the proportional term will increase the response speed of the control system. **Integral term**: The function of the integral term is to sum the error over time so that even a small error will cause integral term to increase slowly. The function of the integral term is to eliminate the residual steady-state error that occurs with a pure proportional term. **Derivative term**: Derivative term is calculated by determining the slope of the error over time. Derivative term is used to reduce the overshoot of the integral term and to improve the controller stability.

In this program PID reads the value of the lock-in amplifier and calculates a deviation from the zero value. After that it adjust the frequency aquired from the signal generator so that the lock-in amplifier is driven back to the zero value. Figure 41 represents a flow chart of the measurement program. After PID program verifies is the frequency change more than 1 Hz, the resolution of the HP 8647A. If the frequency change is smaller than 1 Hz program does not write new value to the signal generator. With this arrangement it is possible to avoid constant frequency adjustment to the signal generator. It is also necessary that program verifies if the resonance frequency is found. This is done so that if Lock-in x value is in range -1E-6 $\leq$ x $\leq$ 1E-6 resonance is found. To enhance the accuracy of the measurement signal averaging is used. This is done in such a way that program calculates an

average from 30 measurements points. Time between two points is adjusted to 1 second. Finally all the values are also plotted and saved to a hard drive.

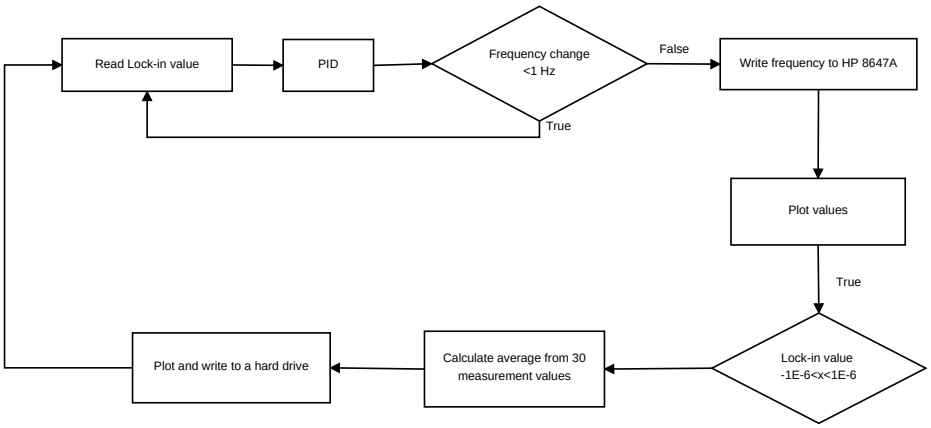

Figure 41. A flow chart of the measurement program

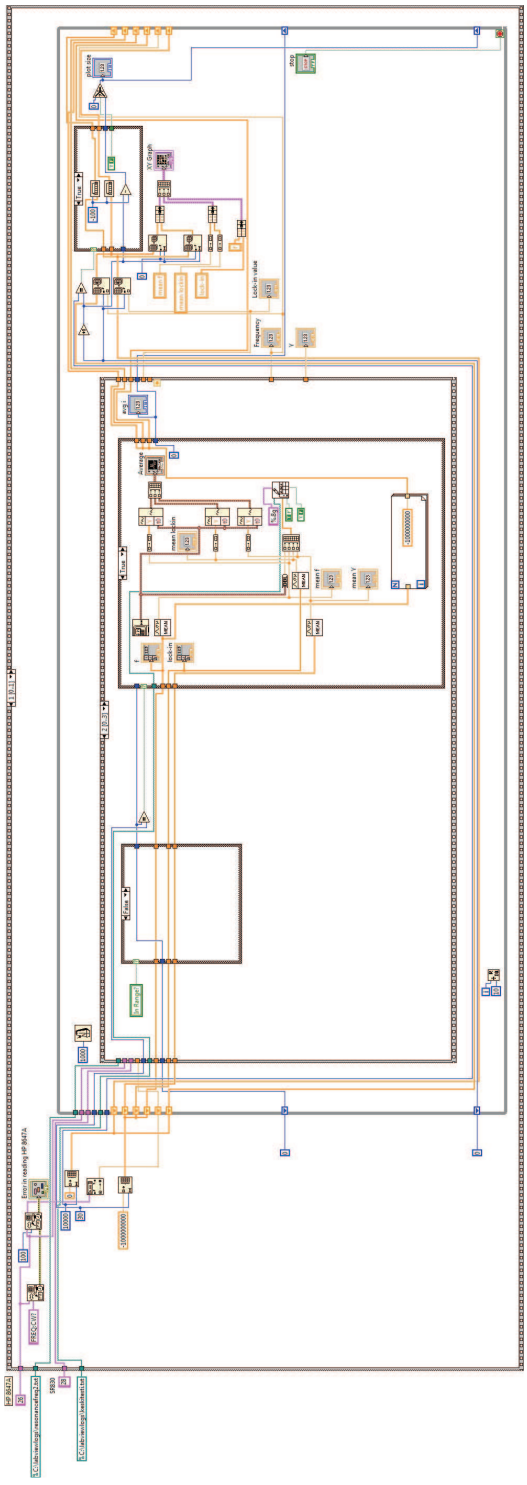

Figure 42. Measurement program

References

[1] G. Sauerbrey, The use of quartz oscillators for weighing thin layers and microweighing (in German), Z. Phys. 155, 206, (1959).

[2] C.K O'Sullivan, G.G Guilbault, Commercial quartz crystal microbalances- theory and application, Biosensors & Bioelectronics 14, 663–670, (1999).

[3] Marvin Chester, L. C. Yang and J. B. Stephens, Quartz Microbalance Studies of an Adsorbed Helium Film, Phys. Rev. Lett. 29, 211–214, (1972).

[4] J. Ahokas, Magnetic Resonance Experiments with Atomic hydrogen, Ph.D thesis, University of Turku, (2010).

[5] Ahmad Safari, E. Koray Akdogan, Piezoelectric and acoustic materials for transducer applications, Springer (2008).

[6] Warren P. Mason, Piezoelectric Crystals and Their Application to Ultrasonics, D. Van Nostrand Company, Inc. Princeton, New Jersey New York (1950).

[7] C.Lu and A.W Czanderna/editors, Application of Piezoelectric Quartz Crystal Microbalances, Elsevier (1984).

[8] David Salt, Handbook of Quartz Crystal Devices, Van Nostrand Reinhold co.Ltd, (1987).

[9] Walter Heywang, Karl Lubitz and Wolfram Wersing, Piezoelectricity Evolution and Future of a Technology, Springer (2008).

[10] J.C. Brice, Crystals for quartz resonators, Rev. Mod. Phys. 57, 105–146, (1985).

[11] Virgile Bottom, Introduction to Quartz Crystal Unit Design, Van Nostrand Reinhold Co. Ltd, (1982).

[12] John. G. Gualtieri, US army Electronics Technology and Devices Laboratory For Monmouth, New Jersey (1989).

[13] V.M. Mecea, From Quartz Crystal Microbalance to Fundamental Principles of Mass Measurements, Analytical Letters, 38, 753–767, (2005).

[14] C.J Wilson, Vibration modes of AT-cut convex quartz resonators, J.Phys. D: Appl. Phys. 7, 2449 (1974).

[15] Ralf Lucklum and Frank Eichelbaum, Interface Circuits for QCM Sensors, Springer Ser. Chem. Sens. Biosens. 5, 3–47, (2007).

[16] Basic Technology of Quartz Crystal Resonators, http://www.4timing.com/techcrystal.htm.

[17] R.Bechmann, Frequency-Temperature-Angle Characteristics of AT-Type Resonators Made of Natural and Synthetic Quartz, Proceedings of the IRE, (1956).

[18] Mitsunori Hieda, Rafael Carcia, Matt Dixon, Tad Daniel, David Allara and M. H. W. Chan, Ultrasensitive quartz crystal microbalance with porous gold electrodes, Appl. Phys. Lett. 84, 628, (2004).

[19] International Crystal Manufacturing Co, Inc, www.icmfg.com/quartzmicrobalance.html.

[20] R.D. Mindlin, Optimal sizes and shapes of electrodes for quartz resonators, J.Acoust. Soc. Am. 43, 1329–1331, (1968).

[21] R.N. Thurston, Allan D. Pierce and Emmanuel P. Papadakis, Ultrasonic Instruments and Devices IIReference for Modern Instrumentation, Techniques and Technology, (1999).

[22] Clemens C. W. Ruppel, Tor A. Fjeldly, Advances in surface acoustic wave technology, systems and applications, volume 2, World Scientific Publishing Co. Pte. Ltd, (2001).

[23] A. EL Habti, F. Bastien, E: Bigler and T. Thorvaldsson, Experimental study of saw quartz resonators at very low temperatures, IEEE ultrasonic symposium, (1995).

[24] Wajid, Abdul, Measuring and controlling deposition on piezoelectric monitor crystal, US patent 5112642, (1992).

[25] Charles P. Poole, Electron Spin Resonance, Interscience publisher, (1967).

[26] Balzers SCD 050 sputter coater operating manual

[27] MORION Inc., www.morion.com.ru

[28] LIT-phonon, www.phonon.msk.ru

[29] Adbellatif El Habti and Francois O. Bastien, Low Temperature Limitation on the Quality Factor of Quartz Resonators, IEEE transactions on ultrasonics, ferroelectrics, and frequency control, 41, 250–255, (1994).

[30] A. Yu. Ivanov and A. M. Plokhotnichenko, A Low-Temperature Quartz Microbalance, Instruments and Experimental Techniques, 52, 308–311, (2009).

[31] J. A. Herb and J. G. Dash, Frequency Dependence of Superfluid Onset in Thin ^{4}He Films, Phys. Rev. Lett. 35, 171–174, (1975).

[32] D.J Bishop and J.D Reppy, Study of the Superfluid Transition in Two-Dimensional ^{4}He Films, Phys. Rev. Lett. 40, 1727–1730, (1978).

[33] J. Krim, J. G. Dash and J. Suzanne, Triple-Point Wetting of Light Molecular Gases on Au(111) Surfaces, Phys. Rev. Lett. 52, 640–643, (1984).

[34] E. Cheng, G. Mistura, H.C. Lee, M.H.W. Chan, M.W. Cole, C. Carraro, W.F. Saam and F. Toigo, Wetting Transitions of Liquid Hydrogen Films, Phys. Rev. Lett. 70, 1854–1857, (1993).

[35] L. Bruschi, G. Delfitto and G. Mistura, Inexpensive but accurate driving circuits for quartz crystal microbalances, Rev. Sci. Instrum. 70, 153, (1999).

[36] J.J. Suter, Piezoelectric properties of quartz crystal resonators below 10 K, Cryogenics, 30, 547–548, (1990).

[37] Balzers QualyTest HLT 260 leak detector operating manual

[38] E.Kim and M.H.W Chan, Observation of superflow in solid helium, Science 305, (2004).

[39] Kaden R. A. Hazzard and Erich J. Mueller, Candidate theories to explain the anomalous spectroscopic signatures of atomic H in molecular H2 crystals, Phys. Rev. B 82, (2010).